



REPUBLIQUE ALGERIENNE DEMOCRATIQUE ET POPULAIRE
MINISTERE DE L'ENSEIGNEMENT SUPERIEUR ET DE LA RECHERCHE SCIENTIFIQUE

UNIVERSITE IBN KHALDOUN - TIARET

MEMOIRE

Présenté à :

FACULTÉ MATHÉMATIQUES ET INFORMATIQUE
DÉPARTEMENT D'INFORMATIQUE

Pour l'obtention du diplôme de :

MASTER

Spécialité : (RT) Réseaux et Télécommunications

Par :

LAZERGUI Abdelkader & BAKEL Abdennasseur

Sur le thème

GaN-based High Electron Mobility Transistors for High Frequency HF Applications

Soutenu publiquement le 13 / 10 / 2021 à Tiaret devant le jury composé de :

Mr DAOUD	Bachir	Grade	Université Tiaret	Président
Mme KERMAS	Nawel	Grade	Université Tiaret	Encadreuse
Mr OUARED	Abdelkader	Grade	Université Tiaret	Examineur

2020-2021

THANKS

*through this modest work, we thank
"ALLAH" for giving us health, courage
and help for the making of this work.*

*We express our deep gratitude to our mentor
Mme. NAWEL KRAMSI for her precious advice and
his supervision in order to carry out this modest work*

*We also extend our sincere thanks
and members*

*Jury :Mr DAOUD Bachir and Mr OUARED Abdelkader
For the honor they have done us to judge and examine
this work Memory*

*At the end of this work, we want to thank the family for
their support*

DEDICATIONS

To my dear parents

To my family

And to my beautiful family

I would like to thank all the people I came to meet during years past, for their sympathy, their generosity, their sincerity, and their good humor because they all contributed to the smooth running of this work.

TABLE OF CONTENTS

GENERALE INTRODUCTION.....	1
CHAPTER I	
I. GAN TECHNOLOGY PROPERTIES.....	3
I.1 .INTRODUCTION.....	3
I.1.1 History of GaN Technology.....	4
I.2 BASIC PROPERTIES OF GAN.....	7
I.2.1 Crystal structure.....	8
I.2.2 Electronic band structure.....	11
I.3 TWO DIMENSIONAL ELECTRON GAS.....	12
I.3.1 Spontaneous & Piezoelectric Polarization.....	13
I.4 APPLICATION AREAS OF GAN.....	16
- LEDs.....	16
- Transistors.....	16
- Radars.....	17
- Nanoscale.....	17
- Spintronics potential[.....	17
I.5 THE III-NITRIDE ALLOYS.....	17
I.6 AL _x GA _{1-x} N/GAN HETEROSTRUCTURE.....	18
I.7 SUMMARY.....	20
CHAPTER II	
II. ALGAN /GAN HIGH ELECTRON MOBILITY TRANSISTORS (HEMTs).....	21
II. 1. INTRODUCTION.....	21
II. 2. HIGH ELECTRON MOBILITY TRANSISTORS (HEMTs).....	22
II. 2.1. BACKGROUND.....	24
II. 2.1.1.HISTORY OF HEMTs.....	25
II. 2.1.2.Working principle of HEMTs.....	27
II. 2.2. Al _x Ga _{1-x} N/GaN HEMTs structure.....	29
II. 2.2.1.GaN-based HEMTs.....	29
II. 3. GROWTH TECHNIQUES AND SUBSTRATES CHOICE.....	33
II. 3.1. SILICON CARBIDE SUBSTRATES (SiC).....	33
II. 3.2. SAPPHIRE SUBSTRATES.....	34
II. 3.3. GAN AND ALN SUBSTRATES.....	35
II .4.HEMTs OPERATION.....	37
II .4.1.DC characteristics.....	39
II .4.2.Degradation of HEMT performance.....	40
II .4.2.1.DEGRADATION MECHANISMS.....	40
II .4.3. BREAKDOWN MECHANISMS.....	42
II. 5 SUMMARY.....	44
CHAPTER III	
SIMULATION RESULTS AND DISCUSSION	
III.2 ABOUT THE SIMULATION SOFTWARE.....	45
III.2.1ATLAS SIMULATION TOOLS (FROM THE COMPANY SILVACO).....	46

1-DEVEDIT.....	47
2-DECKBUILD.....	47
5-OPTIMIZE.....	48
III.2.2 THE MESH:.....	49
III.2.3 THE SUBSTRATE AND THE DOPING.....	49
III.2.4. THE PROGRAMMING STEPS:.....	50
III.3- ANALYTICAL CURRENT MODEL.....	51
III.3-1 –ANALYTICAL CURRENT MODEL.....	52
III.3.2..MODEL DESCRIPTION.....	52
A.SURFACE POTENTIAL.....	52
B. CHARGES.....	52
C. DRAIN CURRENT.....	53
D. ACCESS REGION RESISTANCE.....	53
E. GATE CURRENT.....	53
F. TEMEPERATURE DEPENDENCE.....	54
G. NOISE MODELS.....	54
III.4 HEMT DEVICE STRUCTURE.....	56
A.MESH.....	56
B.. THE REGIONS.....	57
C..ELECTRODS.....	57
D..DOPING.....	57
III.5 IV CHARACTERISTICS.....	58
III.5 .1.GATE CHARACTERIZATION.....	58
III.6. RESULTS AND DISCUSSION.....	59
III.6.1.DESCRPTION OF THE SIMULATED STRUCTURE.....	59
III.7. CONCLUSION.....	64

CHAPTER IV

CONCLUSION AND FUTURE WORK PROSPECTS

IV.1 GENERAL CONCLUSION.....	65
IV.2 FUTURE WORK PROSPECTS.....	66
III.7-REFERENCE.....	67

LIST OF TABLE

TABLE I. 1.FUNDAMENTAL PROPERTIES OF SILICON, SiC, AND GAN MATERIALS	4
TABLE I. 2.REPORTS THE MAIN PHYSICAL PROPERTIES OF GAN	7
TABLE I. 3. VARIOUS IMPORTANT CRYSTAL PLANES OF WURTZITE GAN ALONG WITH THEIR MILLER INDICES AND	11
TABLE I. 4.SPONTANEOUS POLARIZATION AND ELASTICITY COEFFICIENTS AND PIEZOELECTRIC	15
TABLE III . 1 LISTE OF SYMBOLS	56

LIST OF FIGURE

FIGURE I.1 .(A) & (B) STRUCTURE OF HCP LATTICE	8
FIGURE I.2. SYMMETRY ELEMENTS OF POINT GROUP 6MM FOR HEXAGONAL GAN	9
FIGURE I.3.D VIEW OF CRYSTALLOGRAPHIC STRUCTURE OF HEXAGONAL GAN.	10
FIGURE I.4.APPLICATION AREAS OF GAN	13
FIGURE I.5. PIEZOELECTRIC AND SPONTANEOUS POLARIZATION FIELDS	16
FIGURE II.1.GENERALIZED ENERGY BAND DIAGRAM OF HEMTs	28
FIGURE II.2.ALGAN/GAN HEMT STRUCTURE.....	30
FIGURE II.3.(A) SIMPLIFIED ALGAAS/GAAs HEMT STRUCTURE, (B) CORRESPONDING BAND DIAGRAM	37
FIGURE II.4.(A) SIMPLIFIED ALGAN/GAN HEMT STRUCTURE, (B) CORRESPONDING BAND DIAGRAM. ..	38
FIGURE II.5. A TYPICAL OUTPUT CHARACTERISTIC OF HEMT DEVICES.	39
FIGURE II.6.SCHEMATIC OF DEGRADATION MECHANISMS IN ALGAN/GAN HEMTs.	41
FIGURE III-1: THE TONYPLOT ENVIRONMENT	48
FIGURE III-2; MESH DEFINITION	49
FIGURE III-3: DEFINITION OF THE SUBSTRATE	50
FIGURE III-3: DOPING OF PHOSPHORUS	50
FIGURE III.4 ATLAS ENTRANCES AND EXITS	51
FIGURE III.5: DRAIN CURRENT (LEFT Y-AXIS) AND GM (RIGHT Y-AXIS) AS A FUNCTION OF GATE VOLTAGE FOR DIFFERENT DRAIN BIASES, RANGING FROM 0V TO 6V IN STEPS OF 0.5V.	54
FIGURE III-6: DEFINITION OF THE MESH	56
FIGURE III-7: DEFINITION OF THE ELECTRODES.	57
FIGURE III-7: DEFINITION OF THE ELECTRODES	57
FIGURE III-25: DEFINITION OF REGIONS	58
FIGURE 15: BAND DIAGRAM OF MODELED ALGAN/GAN HEMT.	59
FIGURE III-1: THE TONYPLOT ENVIRONMENT	52
FIGURE III-2; MESH DEFINITION	53
FIGURE III-3: DEFINITION OF THE SUBSTRATE.....	54

FIGURE III-3: DOPING OF PHOSPHORUS	54
FIGURE III.4 ATLAS ENTRANCES AND EXITS	55
FIGURE. III.5 HETEROSTRUCTURE INTERFACE AND ENERGY BAND PROFILE OF AN ALGAN/GANHEMT.	57
FIGURE II.5: MESH OF OUR STRUCTURE	62
FIGURE III.6: REGIONS OF OUR STRUCTURE	62
FIGURE III.7: ELECTRODES OF OUR STRUCTURE	63
FIGURE III.8 THE STRUCTURE OF HEMT AL _{0.30} GA _{0.70} N / GAN SIMULATED BY ATLAS-SILVACO, ON THE LEFT THE REPRESENTATION OF THE DIFFERENT REGIONS AND ON THE RIGHT THE REPRESENTATION IS MADE ACCORDING TO THE TYPE OF MATERIAL.	64
FIGURE III.9: THE DRAIN CURRENT-DRAIN VOLTAGE CHARACTERISTICS FOR GATE VOLTAGES	65
FIGURE III 10: THE OUTPUT DROP RETURN POINT (V _{DS}) OF A HEMT TRANSISTOR	
FIGURE III.11: EVOLUTION OF THE NETWORK TEMPERATURE IN THE COMPONENT FOR V _{GS} = 0 AND -2 V INFLUENCE OF THE SUBSTRATE (A) 4H-SiC, I _{DS} -V _{DS} OUTPUT CHARACTERISTICS FOR V _{GS} = 0 AND -2 V.	67
FIGURE III-11 EFFECT OF GEOMETRIC PARAMETERS ON THE CHARACTERISTICS OF THE HEMT TO GAN	68

ABBREVIATIONS

2DEG	Two Dimensional Electron Gas
AlGa _N	Aluminum Gallium Nitride
AlN	Aluminum Nitride
CMOS	Complementary Metal Oxide Semiconductor
FET	Field Effect Transistors
GaAs	Gallium Arsenide
GaN	Gallium Nitride
HBT	Heterostructure Bipolar Transistor
HCP	Hexagonal Closed Pack
HEMT	High Electron Mobility Transistors
InN	Indium Nitride
MBE	Molecular Beam Epitaxy
MESFET	Metal-Semiconductor Field Effect Transistors
MISFET	Metal-Insulator Field Effect Transistors
MOCVD	Metal Organic Chemical Vapor Deposition
MODFET	Modulation Doped FET
Rf	Radio-Frequency
SAW	Surface Acoustic Wave
SET	Single Electron Transistors
SIA	Semiconductor Industry Association
SiC	Silicon Carbide

المخلص

في الآونة الأخيرة ، يمكن للترانزستورات عالية الحركة الإلكترونية القائمة على نيتريد الغاليوم (HEMTs) التنافس مع ترانزستورات LDMOS القائمة على السيليكون (Si) و pHEMTs القائمة على زرنيخيد الغاليوم (GaAs) في السوق. المحطات الأساسية المستخدمة للاتصالات (3G ، 4G ، WiMAX ، ...) جعل التقدم التكنولوجي الذي تم إحرازه في السنوات الأخيرة من الممكن الحصول على ترانزستورات سريعة ذات خصائص مثيرة للاهتمام. يتطلب تصميم الدوائر للأنظمة المعقدة كثافة تكامل عالية ، وهذا يتطلب معالجة التأثيرات الحرارية المرتبطة بتبديد الطاقة العالية والمسؤولة عن تدهور أداء هذه الأنظمة. يركز العمل المقدم في هذه الأطروحة على دراسة التأثير الحراري على سلوك التيار المستمر لترانزستور HEMT في تقنية الجاليوم. في هذا السياق ، تم تطوير نموذج فيزيائي حراري ناتج عن اقتران نموذج انتشار الانجراف ونموذج حراري يعتمد على طريقة العناصر المحدودة لهذا الترانزستور. يأخذ هذا النموذج في الاعتبار درجة حرارة الشبكة في أي نقطة من المكون. يسمح بالدراسة والتحليل التفصيلي لتأثير درجة الحرارة على جميع معاملات هذا المكون. تم استخدام هذا النموذج لفحص تأثير بعض المعلمات التكنولوجيات التي تؤثر على أداء الترانزستور مثل طول البوابة والحاجز وسمك الركيزة.

Abstract

Recently, high electron mobility transistors (HEMTs) based on gallium nitride (GaN) are able to compete the LDMOS transistors based on silicon (Si) and pHEMTs based on gallium arsenide (GaAs) on market base stations used for telecommunications (3G, 4G, WiMAX, ...). Technological advances in recent years have used to fast transistors with interesting features. Circuit design for complex systems require high integration density, this requires treating the thermal effects associated with high power dissipation and are responsible for the degradation of the performance of these systems. The work presented in this thesis focuses on the study of the thermal effect on the DC behavior of GaN HEMT technology. In this context, a physical model from a thermal coupling of a drift-diffusion model and a thermal and based on the finite element model was developed for this transistor. This model takes into account the temperature at any point of the network component. It allows the study and detailed analysis of the effect of temperature on all the parameters of the component. This model was used to examine the influence of some technological parameters that affect the performance of the transistor such as gate length, the thickness of the gate and the substrate.

Résumé

Récemment, les transistors à haute mobilité électronique (HEMTs) à base de nitrure de gallium (GaN) sont capables de concurrencer les transistors LDMOS à base de silicium (Si) et les pHEMTs à base d'arséniure de gallium (GaAs) sur le marché des stations de bases utilisées pour les télécommunications (3G, 4G, WiMAX,...). Les progrès technologiques accomplis ces dernières années permettent de disposer des transistors rapides ayant des caractéristiques intéressantes. La conception des circuits pour les systèmes complexes nécessitent une grande densité d'intégration, ceci impose de traiter les effets thermiques liés aux fortes dissipations de puissances et qui sont responsables de la dégradation des performances de ces systèmes. Le travail présenté dans ce mémoire porte sur l'étude de l'effet thermique sur le comportement DC du transistor HEMT en technologie GaN. Dans ce cadre, un modèle physico-thermique issu d'un couplage d'un modèle de dérive-diffusion et d'un modèle thermique est basé sur la méthode des éléments finis a été développé pour ce transistor. Ce modèle prend en compte la température de réseau en tout point du composant. Il permet l'étude et l'analyse détaillée de l'effet de la température sur l'ensemble des paramètres de ce composant. Ce modèle a été exploité pour examiner l'influence de certains paramètres technologiques qui impactent les performances du transistor tels que la longueur de la grille, l'épaisseur de la barrière et du substrat.

GENERAL INTRODUCTION

In recent years, the development of III-V compounds has been spectacular. In fact, these compounds exhibit much better performance than those more traditional semiconductors such as silicon. These are the materials of choice for all microelectronic and optoelectronic applications. However, the characteristics of these materials and their components are sensitive to surface finish and interface. The study of operation of the different types of electronic components requires a mastery prerequisite of the physical phenomena governing the properties of electrons in the semiconductor. It is therefore essential to understand the mechanisms of formation of heterostructures and nanostructures to better master component technology achieved, at a time when nanotechnologies are opening up new avenues.

Indeed, the interest in III-V compounds such as gallium arsenide (GaAs) or Gallium nitride (GaN) has been spectacular. However, nowadays microelectronics and optoelectronics are constantly developing and many studies are being carried out to have ever more efficient semiconductors.

Gallium nitride (GaN) admits a wide and direct forbidden band, a large chemical and thermal stability, very good mechanical properties, and properties very interesting physics to operate at high temperature, high power and high frequency.

It shows great promise for applications in microelectronics and in optoelectronics. Possibly combined with other III-V compounds, it makes it possible to produce various devices for a very wide range of applications, including HEMT transistors.

In addition to these physical properties, GaN has the particularity of being a material pyroelectric and piezoelectric. This specificity makes it possible to produce HEMT transistors AlGaN / GaN type whose interface electron density can easily exceed 1.10^{13}cm^{-2} without intentional doping of the AlGaN barrier.

However, the manufacturing processes used for HEMT AlGaN / GaN are complex and lead to the formation of numerous crystal defects. Parasitic effects of functioning are induced by physical mechanisms that penalize the transport of carriers in the structure.

At present, these parasitic effects have a negative influence on the performance of these transistors. They are mainly related to electron traps induced by impurities present in the material or crystalline defects.

In the first chapter; we treat III-V semiconductors in a way general, and gallium nitride in particular. [1]

CHAPTER I

GaN technology Properties

I. GaN technology Properties

I.1 .Introduction

Gallium nitride (GaN) is a very hard, mechanically stable wide bandgap semiconductor. With higher breakdown strength, faster switching speed, higher thermal conductivity and lower on-resistance, power devices based on GaN significantly outperform silicon-based devices. Gallium nitride crystals can be grown on a variety of substrates, including sapphire, silicon carbide (SiC) and silicon (Si). By growing a GaN layer on top of silicon, the existing silicon manufacturing infrastructure can be used eliminating the need for costly specialized production sites and leveraging readily available large diameter silicon wafers at low cost.^[02]

The material, which we call “semiconductor”, has a rich and interesting history that begins from 1833, when Michael Faraday discovered that semiconductor electrical conductivity increases with increase in temperature . This behavior of semiconductor was different from the behavior exerted by metals, where conductivity decreases with increase in temperature. The progress was slow until 1948, when point contact devices were first introduced leading to the use of silicon extensively. The history of information theory was made by silicon because of its excellent characteristics. Silicon products have evolved over time and considered as a carrier of information for a long time. It has played a tremendous role in the development of high performance electronic devices, which are part of our everyday lives Silicon is the heart of conventional computer-based technology. From our cell phones, super-fast computers to high-tech cars, most of the technology we enjoy today is because of the enormous development in computing. This advancement was possible because of the growth in the transistor industry.

Researchers have seriously started to figure out new methods to shrink the size of transistors as well as increase the processing speed higher than ever before. The performance of silicon devices is limited for today’s requirements because of inherent

limitations of its properties Computing power cannot sustain its exponential growth by relying on silicon anymore. Moreover, silicon has reached its theoretical limit in power conversion. It cannot In the last few years, gallium nitride (GaN) and silicon carbide (SiC) have been receiving much attention. Also, SiC and GaN semiconductors are commonly attributed as compound semiconductors because they are comprised of multiple elements from different groups in the periodic Table I. 1. These materials have challenged the long held dominance of silicon. ^[03]

Table I. 2.Fundamental properties of silicon, silicon carbide, and gallium nitride materials

Property	Si	SiC	GaN
Bandgp Energy eV	1.12	3.2	3.39
Electron mobility $\text{cm}^2/\text{V.s}$	1360	950	2000
Breakdown field MV/cm	0.23	2.2	3.3

I.1.1 History of GaN Technology

Literature on the growth of nitrides based research dates back in early 60s. Since then, nitride technology has always lagged behind the easier to grow Si and GaAs based studies. The first systematic effort to grow InN, GaN and AlN by chemical vapour deposition or sputtering processes took place in the 1970s with the emphasis on characterization of structural and optical properties. The III nitride materials got serious attention in late 80s. In the early research, metalorganic precursors containing In or Al with electronic grade purity were not available, As a result substantial defect concentration and high n-type background was unavoidable in the growth of GaN films. A large concentration of free electrons was presumed to result from oxygen impurities and intrinsic defects. Films having relatively small

background electron concentration or p-type doping could not be achieved even until recently. Also, substrate material with reasonably good thermal and lattice matches to the nitrides were not available. AlN was one of the options but the structural quality of the AlN films was not good enough for optical or electronic applications. All these problems resulted in late coming of technological spin-offs, only after some of these problems were addressed with reasonable success. Large single crystal GaN substrate is not available commercially. This presents a key problem in the growth of homoepitaxial GaN films, making heteroepitaxy a necessity; consequently a suitable choice of substrate becomes crucial. Most often, the lattice constant mismatch has been the primary criterion for determining the suitability of a material as a substrate for GaN epitaxy however other properties are also important, such as crystal structure, thermal expansion coefficient, chemical, and electrical properties, composition, reactivity, and surface finish.

The substrate employed determines the crystal orientation, polarity, polytype, the surface morphology, strain, and the defect concentration of the GaN film, ultimately determining the optimal device performance. There are few techniques which can be employed to ameliorate some of the shortcomings of the substrate. Appropriate surface preparation such as nitridation, pendeoepitaxy, epitaxial lateral overgrowth, deposition of a low-temperature AlN or GaN buffer layer, multiple intervening low-temperature buffer layers, and other techniques have been employed for this purpose. Sapphire (Al_2O_3) and SiC are the most popular substrate materials used currently, although, recently a few groups have reported using Si as a substrate material for GaN film growth, in the drive to make it cheaper and Si compatible. The residual strain due to lattice misfit in GaN on sapphire is comparable to the strain due to misfit between 6H-SiC and GaN, as a result comparable dislocation densities have been observed. GaN layers with dislocation densities as low as 10^7 cm^{-2} have been produced but even lower defect densities are necessary for more sophisticated devices operating at more extreme conditions of temperature, voltages, and current densities. Thus far, the (0 0 0 1) sapphire are the

most commonly used substrates for the growth of GaN, as this orientation is generally the most favorable for growing smooth films. However, interest in GaN epitaxial layers with other orientations is also increasing to eliminate the polarization effects as such effects can be deleterious for some optoelectronic applications, in which piezoelectric effects in quantum wells can cause a spatial separation of electrons and holes, thereby decreasing the recombination efficiency [30].

Many epitaxial thin film growth processes have been developed, including molecular beam epitaxy (MBE), hydride vapor phase epitaxy (HVPE), supersonic jet epitaxy [31], and metalorganic chemical vapor deposition (MOCVD). Some combined and derivative techniques have also been tried to exploit the benefit of the individual technique. For example metalorganic molecular beam epitaxy (MOMBE), which combines the MOCVD and MBE technique in the same growth machine. Primarily, the development of MOCVD and plasma-induced molecular beam epitaxy (PIMBE) over the last eight years has led to a number of recent advances and important improvements in structural properties. As a result it could be possible to achieve few successful applications based on GaN. One such remarkable application is the achievement of super-bright blue LEDs which were fabricated by MOCVD method. High growth rates, high purity chemical sources, large scale manufacturing potential and the ability to grow abrupt junctions, and a high degree of composition control and uniformity, all these are characteristics of MOCVD that made it possible. [34]

I.2 Basic properties of GaN

GaN is a very hard, mechanically stable wide-bandgap semiconductor material with high heat capacity and thermal conductivity. In its pure form it resists cracking and can be deposited in thin film on sapphire or silicon carbide, despite the mismatch in their lattice constants.

GaN can be doped with silicon (Si) or with oxygen to n-type and with magnesium (Mg) to p-type. However, the Si and Mg atoms change the way the GaN crystals grow, introducing tensile stresses and making them brittle.

Gallium nitride compounds also tend to have a high dislocation density, on the order of 10^8 to 10^{10} defects per square centimeter.

The wide band-gap behavior of GaN is connected to specific changes in the electronic band structure, charge occupation and chemical bond regions.

The U.S. Army Research Laboratory (ARL) provided the first measurement of the high field electron velocity in GaN in 1999. Scientists at ARL experimentally obtained a peak steady-state velocity of 1.9×10^7 cm/s, with a transit time of 2.5 picoseconds, attained at an electric field of 225 kV/cm. With this information, the electron mobility was calculated, thus providing data for the design of GaN devices. ^[05]

Table I. 3.reports the main physical properties of GaN

Properties	
Chemical formula	GaN
Molar mass	83.730 g/mol
Appearance	yellow powder
Density	6.1 g/cm ³
Melting point	>1600 °C
Band gap	3.4 eV (300 K, direct)
Electron mobility	1500 cm ² /(V·s) (300 K)
Thermal conductivity	1.3 W/(cm·K) (300 K)
Refractive index (nD)	2.429

I.2.1 Crystal structure

The GaN bond in gallium nitride crystal is strongly ionic and the bonding energy is 8.9 eV. The strong ionic bond makes gallium nitride very stable and has a melting point of 2500 o C [Van Vechten, 1973]. Gallium nitride has two different crystal structures. The normally stable structure is hexagonal close-packed (HCP) structure which is one of the two ways where spheres can be packed together in space with the greatest possible density and still have a periodic arrangement. The structure is shown in **Figure I. 1 . (a)**. There are two lattice points per unit cell, one is at (0,0,0) and the other one is at ($2/1, 3/1, 3/2$) or ($2/1, 3/2, 3/1$), which is equivalent). Another representation of the HCP structure is shown in **Figure I.1 . (b)**, the three atoms in the interior of the hexagonal prism are directly above the centers of the alternate triangle in the base. The lattice parameter of HCP GaN is $a_1 = a_2 = 3.1887 \text{ \AA}$, $c = 5.1853 \text{ \AA}$. The ratio of c/a is 1.626, which is very close to the standard c/a ratio of 1.633 for hexagonal lattice made of spheres.

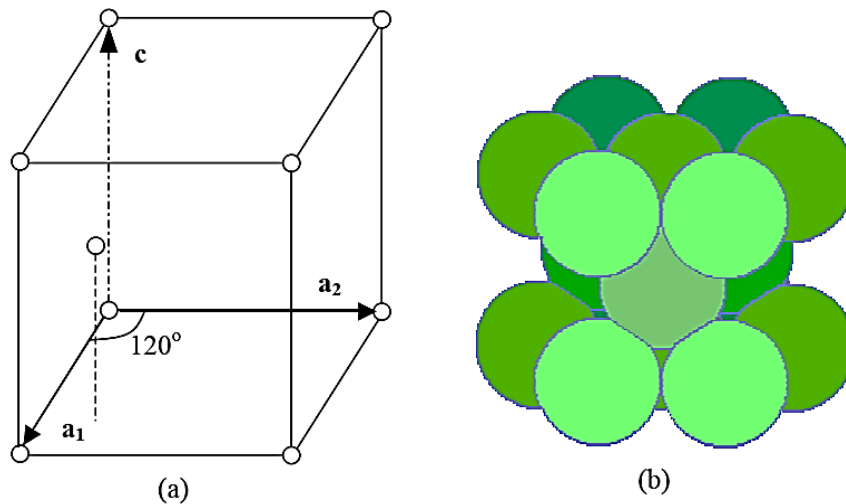


Figure I.1 .(a) & (b) Structure of HCP lattice

As seen in **Figure I.1 . (a)**, the HCP structure of gallium nitride belongs to the primitive hexagonal lattice with $a_1 = a_2 \neq c$, $\alpha = \beta = 90^\circ$, $\gamma = 120^\circ$ According to the

Pearson symbol [Pearson, 1967] which indicates the crystal symmetry and the number of atoms in the unit cell, the HCP structure for GaN is designated as hP4.

The “h” means “hexagonal”, the capital “P” indicates that the centering is “primitive”, the number “4” stands for the number of atoms in the unit cell of wurtzite GaN. The point group representing the symmetry in two-dimensional lattice for GaN hexagonal lattice is 6mm. The “6” means 6-fold rotational axial symmetry with the axis of rotation perpendicular to the plane of the two-dimensional lattice. The axis is the C-axis in the three-dimensional lattice. The both letters “m” indicates the presence of the mirror reflection symmetry with two mirror planes (lines in two dimensions) parallel to the rotational c-axis. The symmetry elements of point group 6mm for hexagonal GaN are shown in **Figure I. 2**

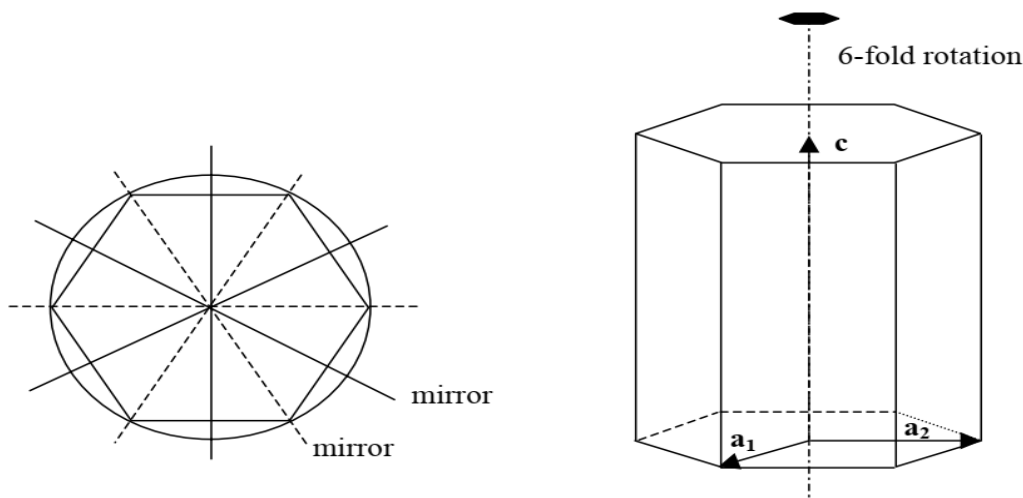


Figure I.2. Symmetry elements of point group 6mm for hexagonal GaN

A space group involves not only rotation, inversion, and reflection symmetry elements, but also translation [Brown & Forsyth, 1973]. A combination of rotation and translation can be thought as a symmetry operation with a screw axis, and a combination of reflection and translation can be viewed as an operation with a glide

plane of symmetry. The three-dimensional space group of hexagonal gallium nitride lattice belongs to P63mc (The No. is 186 among total of 230). The capital letter “P” is for “primitive”. The latter combination of the numbers and letters displays the fact that translation and glide elements are added for a space description of the lattice. The “63” indicates that there is a repetition through rotation on $360/6 = 60^\circ$ and translation of $3/6c = c/2$. The notation “mc” represents the fact that in three-dimensional sense of the space group, one of the mirror planes has been replaced by the glide plane, which is parallel to the repeat vector c . For compound GaN with both Ga atoms and N atoms, there are gallium atoms both at $(0,0,0)$ and at $(2/3,1/3,1/2)$. Nitrogen atoms are located at $(0,0,u)$ and $(2/3,1/3,1/2+u)$, where u is 0.377, which approximately equals to $3/8$. The 3-D view of crystallographic structure of GaN using online software Webemaps [Zuo & Mabon, UIUC] is shown in **Figure I. 3**

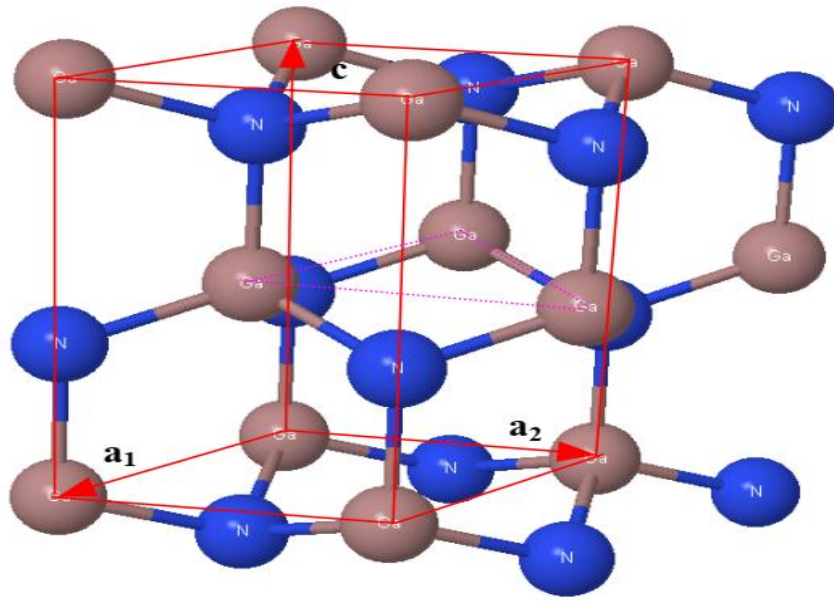


Figure I.3.D view of crystallographic structure of hexagonal GaN.

Another structure of GaN is the face-centered cubic (FCC) structure which is equally closed packed arrangement with HCP structure. The atoms on the (111) planes

of the FCC structure are arranged in a hexagonal pattern just like those atoms on the (0002) planes of the HCP structure. The difference is that the atoms on the third layer are directly above those on the first layer with stacking sequence of ABABA^[06]

Table I. 4. Various important crystal planes of wurtzite GaN along with their miller indices and

Plane	Index	Polarity
c – Plane	(0001)	Polar
a – Plane	(11–20)	non-polar
m – Plane	(10 –10)	non-polar
r – Plane	(1–102)	semi-polar

GaN was conventionally grown along c-plane to utilize the associated polarization for electronic applications. However, polarization induced fields have been found to limit optical device performances due to which fabrication of optical devices on non-polar and semi-polar GaN has garnered more attention

I.2.2 Electronic band structure

In solid-state physics, the electronic band structure (or simply band structure) of a solid describes the range of energy levels that electrons may have within it, as well as the ranges of energy that they may not have (called band gaps or forbidden bands).

Band theory derives these bands and band gaps by examining the allowed quantum mechanical wave functions for an electron in a large, periodic lattice of atoms or molecules. Band theory has been successfully used to explain many physical properties of solids, such as electrical resistivity and optical absorption, and forms the foundation of the understanding of all solid-state devices (transistors, solar cells, etc.)

The electrons of a single, isolated atom occupy atomic orbitals each of which has a discrete energy level, when two or more atoms join together to form a molecule, their atomic orbitals overlap.

The Pauli Exclusion Principle dictates that no two electrons can have the same quantum numbers in a molecule. So if two identical atoms combine to form a diatomic molecule, each atomic orbital splits into two molecular orbitals of different energy, allowing the electrons in the former atomic orbitals to occupy the new orbital structure without any having the same energy.

Similarly if a large number N of identical atoms come together to form a solid, such as a crystal lattice, the atoms' atomic orbitals overlap. Since the Pauli Exclusion Principle dictates that no two electrons in the solid have the same quantum numbers, each atomic orbital splits into N discrete molecular orbitals, each with a different energy. Since the number of atoms in a macroscopic piece of solid is a very large number ($N \sim 10^{22}$) the number of orbitals is very large and thus they are very closely spaced in energy (of the order of 10^{-22} eV). The energy of adjacent levels is so close together that they can be considered as a continuum, an energy band.^[07]

I.3 Two Dimensional Electron Gas

A two-dimensional electron gas (2DEG) is a scientific model in solid-state physics. It is an electron gas that is free to move in two dimensions, but tightly confined in the third. This tight confinement leads to quantized energy levels for motion in the third direction, which can then be ignored for most problems. Thus the electrons appear to be a 2D sheet embedded in a 3D world. The analogous construct of holes is called a two-dimensional hole gas (2DHG), and such systems have many useful and interesting properties. Most 2DEGs are found in transistor-like structures made from semiconductors.

2DEG is a valuable system for exploring the physics of superconductivity magnetism and their coexistence.

The need for attaining new functionalities in modern electronic devices has led to the manipulation of property of an electron called spin degree of freedom along with its charge. This has given rise to an altogether new field of spin-electronics or 'spintronics'.

The manipulation of electron spin offers new dimensions for basic and applied research, and the potential for new capabilities for electronics technology. This motivates studies of spin polarized electrons in a high mobility two dimensional electron gas (2DEG). [08]

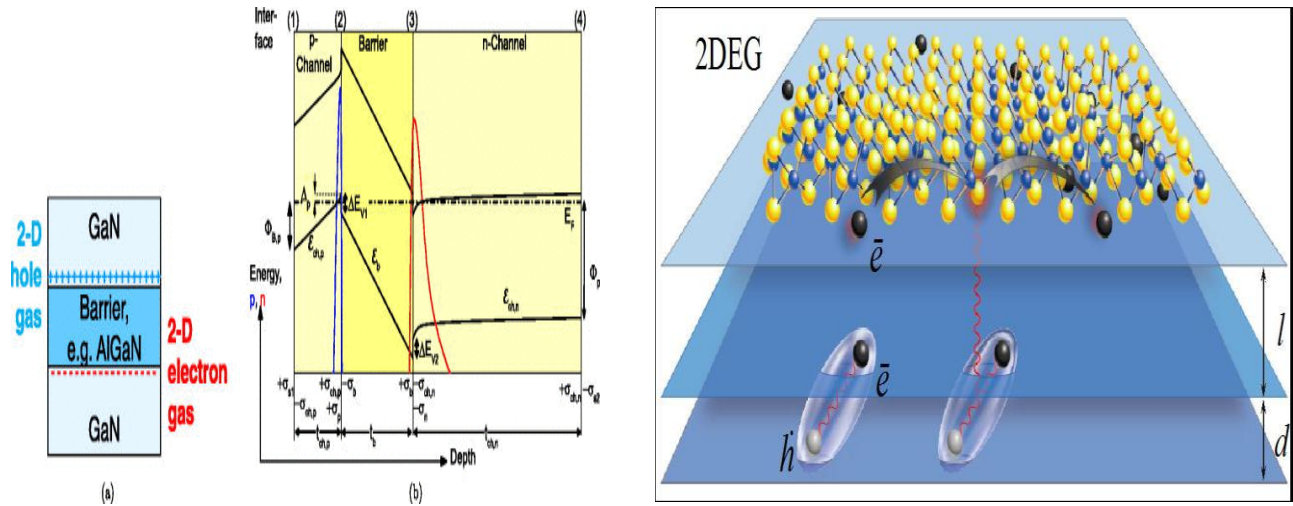


Figure I.4. Application Areas of GaN

I.3.1 Spontaneous & Piezoelectric Polarization

The role of spontaneous and piezoelectric polarization in III–V nitride heterostructures is investigated. Polarization effects and crystal polarity are reviewed in the context of nitride heterostructure materials and device design, and a detailed analysis of their influence in nitride heterostructure field-effect transistors is presented. The combined effects of spontaneous and piezoelectric polarization are found to account well for carrier concentrations observed in AlGaIn/ GaN transistor structures with low to moderate Al concentrations, while the data for higher Al concentrations are consistent with defect formation in the AlGaIn barrier. Theoretical analysis suggests that incorporation of In into the barrier and/or channel layers can substantially increase polarization charge at the heterojunction interface. The use of polarization effects to engineer Schottky barrier structures with large enhancements in barrier height is also discussed, and electrical characteristics of transistors with conventional and

polarization-enhanced Schottky barrier gates are presented. The polarization-enhanced barrier is found to yield a marked reduction in gate leakage current, but to have little effect on transistor breakdown voltage. [09]

The strong spontaneous polarization and piezoelectric effects in the wurtzite III nitride semiconductors lead to new possibilities for device design. In typical heterojunction field effect transistors these effects are used to create large electron concentrations at the AlGaN/GaN interface. However, we examine several other possible device structures which include heterojunctions of AlGaN, GaN, and InGaN. For example, we find the strong electric fields present in these structures allow us to create quantum wells greater than 1 eV deep. Both Ga-faced and N-faced materials are explored. The two-dimensional electron gas concentrations in these structures are found using a self-consistent 1-D Schrödinger-Poisson solver modified to incorporate the effects of spontaneous and piezoelectric polarization. The boundary conditions at the heterojunction interfaces and at the surface and substrate are discussed in detail. Electron concentrations are compared with those obtained experimentally through capacitance-voltage and Hall effect measurements. [10]

Due to the ionic nature of the metal-nitrogen bond and the absence of a center inversion, hexagonal phase nitrides (wurtzite) are characterized by the presence of a intense internal polarization which consists of two contributions: spontaneous polarization and piezoelectric polarization. The barycenters of positive (carried by metal atoms) and negative charges (carried by nitrogen atoms) do not coincide in the elemental cell of wurtzite and form a set of electric dipoles oriented along the c axis. Thus, a polarization macroscopic electrical power appears, even in an ideal wurtzite structure . phenomenon exists in the crystal at equilibrium in the absence of any external stress. Bernardini et al. show that the spontaneous polarization in nitrides is very high. This spontaneous polarization P_{sp} manifests itself at the interfaces of the material with the vacuum or with another material of a different nature. It creates a monopolar load [P_{sp} .n] at the

interface between the material and the vacuum, or $[P_{sp}(A) - P_{sp}(B)] \cdot n$ at the interface between two materials A and B (n : unit vector normal to the surface).

In all element III nitrides, the polarization vector P_{sp} is oriented following direction [0001]. There are no absolute experimental measurements of the spontaneous polarization in nitrides. Only an ab-initio calculation, developed by Bernardini and al. give numerical values of P_{sp} which is represented in table 4. Spontaneous polarization does not exist in cubic phase semiconductors by reason for symmetry. On the other hand, the action of a bi-axial stress exerted in the plane (111) breaks the cubic symmetry and reveals a polarization oriented along the axis z . This phenomenon is known as piezoelectricity. A piezoelectric polarization occurs also manifested in wurtzite phase semiconductors when a stress is placed on them applied. The application of a constraint which varies the distance between the barycenters of positive and negative charge in the elementary cell. The macroscopic polarization obtained is proportional to the strain, $P_i^{pe} = \sum_j e_{ij} E_j$ where e_{ij} is the piezoelectric tensor. For a material subjected to a biaxial stress e_{xx} in the plane (0001), the polarization piezoelectric is given by $P_{pz} = 2d_{31} \times [C_{11} + C_{12} - 2C_{33}^2 / C_{33}] \times e_{xx}$ where d is the piezoelectric coefficient and the C_{ij} are the elastic constants. Table I.4 gives the values of the elasticity coefficients and the coefficients piezoelectric for GaN, AlN and InN

Table I.5. Spontaneous polarization and elasticity coefficients and piezoelectric

	GaN	AlN	InN
$P(\text{c/m}^2)$	-0.029	108	-0.032
$C_{13}(\text{GPa})$	106	373	92
$C_{33}(\text{GPa})$	389	373	224
$e_{31}(\text{c/m}^2)$	-0.35	-0.5	-0.57
$e_{33}(\text{c/m}^2)$	1.27	1.27	1.57

In element III nitrides, the total polarization of the medium is therefore the sum algebraic of two contributions, one existing at equilibrium (spontaneous polarization), the other under the action of an external stress (piezoelectric polarization) **Figure I.5**

These two polarizations being of the same physical nature, it is very difficult to determine experimentally the contribution of each of them. ^[11]

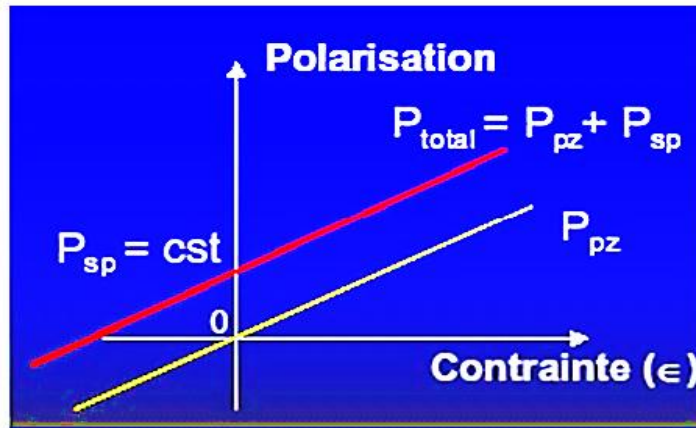


Figure I.5. Piezoelectric and spontaneous polarization fields

I.4 Application Areas of GaN

GaN is used in the production of semiconductor power devices as well as RF components and light-emitting diodes (LEDs).

GaN has demonstrated the capability to be the displacement technology for silicon semiconductors in power conversion, RF, and analog applications.

- LEDs

The mixture of GaN with In (InGaN) or Al (AlGaN) with a band gap dependent on ratio of In or Al to GaN allows the manufacture of light-emitting diodes (LEDs) with colors that can go from red to ultra-violet

- Transistors

GaN transistors are suitable for high frequency, high voltage, high temperature and high efficiency applications.

- **Radars**

They are also utilized in military electronics such as active electronically scanned array radars

- **Nanoscale**

GaN nanotubes and nanowires are proposed for applications in nanoscale electronics, optoelectronics and biochemical-sensing applications.

- **Spintronics potential**

When doped with a suitable transition metal such as manganese, GaN is a promising spintronics material (magnetic semiconductors).

Some of the benefits in the GaN compound that can be used in devices generally include. Lower energy costs: Less energy is expended as heat, which results in materials that are less costly and systems that can be scaled down in size. This is mainly due to the fact that GaN semiconductors are more efficient than silicon.

Power density is higher: Higher switching frequencies than silicon in addition to operational temperatures contribute to smaller heat sinks, lower cooling requirements, liquid-cooling to air cooling conversion, elimination of fans and a cut back on magnetics.

Less costly system: Even though GaN semiconductors are more expensive than silicon, the cost reduction is a result of smaller size/costs of other components such as filters, cooling, passive inductive and capacitive circuit elements.

Higher switching frequencies: Since GaN devices have higher switching frequencies, smaller inductors and capacitors can be used in power circuits. Both the inductance and capacitance are scaled down to match the frequency, where a 10x frequency increase produces a 10x decrease in the capacitance and inductance. As a result, the weight, cost, and volume are all significantly decreased. High frequency also has the potential to create less noise in motor drive applications. . [12]

I.5 The III-nitride alloys

III-Nitrides alloys (GaN, InGaN, AlGaN and AlInGaN) are widely used for several

applications, such as High Electron Mobility Transistors (HEMT), solar cells, light emitting devices. These alloys show a bandgap tunable with composition, covering the whole visible spectrum; however, these materials suffer from the presence of structural defects emerging from strain and thermal relaxation phenomena. We study transport properties, optical spectra, electrical properties at macro and nano-scale and quantum confinement effects in order to clarify the role of material properties on device behaviour.

The III-Nitrides materials system has impacted energy efficiency on the worldwide scale through its application to blue light-emitting diodes (LEDs). This impact on technology and society was recognized by the award of the 2014 Nobel Prize in Physics to Isamu Akasaki, Hiroshi Amano, and Shuji Nakamura. The binary nitrides cover a wide range of direct band gap energies with energy gap tunable by alloy composition ranging from 0.65 eV (InN) to 6.0 eV (AlN). However, the large mismatch in lattice constants between the nitrides and their substrates results in highly strained heterostructures with ternary alloys. This strain can lead to defect formation, reduced material quality, and polarization-related electric fields in basal plane growth.^[13]

I.6 Al_xGa_{1-x}N/GaN heterostructure

the Al_xGa_{1-x}N/GaN heterostructure field-effect transistors (HFETs) for high-power high-temperature and microwave applications have developed rapidly. A good understanding of the transport properties of two-dimensional electron gas (2DEG)

at the Al_xGa_{1-x}N/GaN interface is the fundamental way to improve the operation behaviours of modulation-doped Al_xGa_{1-x}N/GaN HFETs. Different from that of the Al_xGa_{1-x}As/GaAs heterostructures due to the large piezoelectric constant of the Al_xGa_{1-x}N materials and the lattice mismatch between Al_xGa_{1-x}N and GaN, the piezoelectric polarization is very strong in an Al_xGa_{1-x}N layer on GaN. It is thought that the piezoelectric polarization of the Al_xGa_{1-x}N barrier is the main factor in determining the

transport properties of the 2DEG at the $\text{Al}_x\text{Ga}_{1-x}\text{N}/\text{GaN}$ heterointerfaces. As we know, the piezoelectric polarization is strongly influenced by the elastic strain relaxation of the $\text{Al}_x\text{Ga}_{1-x}\text{N}$ layer. The relaxation is determined by the thickness of the $\text{Al}_x\text{Ga}_{1-x}\text{N}$ layer.

The modulation-doped $\text{Al}_x\text{Ga}_{1-x}\text{N}/\text{GaN}$ heterostructures with different $\text{Al}_x\text{Ga}_{1-x}\text{N}$ barrier thicknesses were deposited. High-resolution x-ray diffraction indicates that the heterostructures are of high quality. The 2DEG mobility is much higher than that of the electrons in GaN films at both 300 K and 77 K. It is found that the partial relaxation of the $\text{Al}_x\text{Ga}_{1-x}\text{N}$ barriers has a strong influence on 2DEG mobility.^[14]

I.7 Summary

Today, the vast majority of power devices are made from silicon. Improving their efficiency is crucial to reduce switching losses and hence lower the CO₂ emission. Unfortunately, power devices based on silicon, are reaching their theoretical limits. Design engineers are now facing the challenge of increasing the ratings of converters in terms of operating voltage, operating temperature and efficiency. The quest for a solution to silicon limitations leads researchers to the doorstep of wide bandgap materials such as Silicon Carbide (SiC) and Gallium nitride (GaN). Compared to silicon, the main benefits of these materials are a good operation over a wide temperature range, high critical electric field and high saturation velocity. Despite the remarkable results obtained by several teams working on Silicon Carbide, SiC must be grown on native substrates which are expensive and relatively small in size. On the other hand, GaN can be grown on silicon substrates which are large and of low cost. Moreover, GaN is better than SiC for creating heterostructures due to their built-in polarization field. Therefore, for devices such as HEMT, GaN is the material of choice.

CHAPTER II

***AlGaN /GaN High Electron Mobility
Transistors (HEMTs).***

II. AlGaN /GaN High Electron Mobility Transistors (HEMTs).

II. 1. Introduction

Thanks to the recent advancements in the growth and fabrication processes, the performance of high electron mobility transistors (HEMTs) based on GaN has significantly improved. The main advantages of using GaN as a material for the realization of HEMTs are ,the high sheet charge density of the two-dimensional electron gas (2DEG), which results in a low on-resistance of the transistors; the high thermal conductivity of GaN , which permits to reach high levels of power dissipation while keeping the channel temperature low; the high breakdown field , which allows to fabricate devices with breakdown voltages in the order of hundreds or thousands of volts, depending on gate–drain spacing and on buffer thickness. These unique features make GaN an almost perfect material for the manufacturing of high power transistors: thanks to the recent efforts of the scientific and industrial communities, GaN-based transistors with breakdown voltages in excess of 1.5–1.9 kV have been recently demonstrated, thus clearing the way for the adoption of HEMTs in power electronics. Moreover, thanks to the low (on-resistance) \times (device capacitance) product, GaN-based power HEMTs can reach high switching frequencies, and can therefore be used for the fabrication of high efficiency power conversion systems: converters with efficiencies in excess of 96–98% have already been demonstrated, thus proving the superiority of GaN with respect to more conventional semiconductors for power electronics.

Despite the high performance of GaN-based HEMTs, the lifetime of these devices can be shorter than expected, due to the existence of a number of physical mechanisms responsible for device degradation. Recent studies demonstrated that GaN HEMTs may degrade due to the following processes: degradation of the gate Schottky junction, induced by off-state stress.

This mechanism induces an increase in the gate leakage current, due to the generation of localized shunt paths in proximity of the gate edge; semi-permanent or permanent degradation due to hot electrons; this mechanism occurs when the devices are operated

in the on-state, and — in most of the cases — results in a decrease in drain current, due to the accumulation of negative charge close to the gate edge and/or in the gate–drain access region. delamination of the passivation, due to the exposure to high temperature/power levels, which may result in additional charge trapping and leakage processes. time-dependent degradation processes, due to the generation of defects within the AlGa_N/Ga_N heterostructure. Besides these mechanisms, power devices operated at high drain voltages may show important breakdown (BD) processes; breakdown consists in a rapid increase in drain current, which occurs — in the off-state — when the drain voltage reaches a critical value. Breakdown may be catastrophic (i.e., induce a sudden failure of the devices); this typically happens when BD measurements are carried out in voltage controlled mode, by increasing the drain voltage until a uncontrollable increase in drain current is triggered. A sustainable breakdown condition can be reached if the measurements are carried out in current-controlled mode.’ by using this method it is possible to separately evaluate the contribution of gate, source, and bulk leakage to the overall BD current, thus extracting information on the physical origin of breakdown for several operating conditions.

As can be understood, breakdown represents an important problem for high power/high voltage HEMTs: for this reason, over the past years several groups have investigated the physical origin of BD,^{9,17–25}) with the aim of developing models to explain this phenomenon, Impact ionization mechanisms, that may induce a significant increase in drain current due to the generation of electron–hole pairs close to the gate. [15]

II. 2. High Electron Mobility Transistors (HEMTs)

A high electron mobility transistor (HEMT) , also known as heterostructure FET (HFET) or modulation-doped FET (MODFET) , is a field-effect transistor incorporating a junction between two materials with different band gaps (i.e. a heterojunction) as the channel instead of a doped region (as is generally the case for

a MOSFET). A commonly used material combination is GaAs with AlGaAs, though there is wide variation, dependent on the application of the device.

Devices incorporating more indium generally show better high-frequency performance, while in recent years, gallium nitride HEMTs have attracted attention due to their high-power performance. Like other FETs, HEMTs are used in integrated circuits as digital on-off switches. FETs can also be used as amplifiers for large amounts of current using a small voltage as a control signal. Both of these uses are made possible by the FET's unique current-voltage characteristics. HEMT transistors are able to operate at higher frequencies than ordinary transistors, up to millimeter wave frequencies, and are used in high-frequency products such as cell phones, satellite television receivers, voltage converters, and radar equipment. They are widely used in satellite receivers, in low power amplifiers and in the defense industry. [16].

The HEMT was first demonstrated by Mimura and colleagues at Fujitsu Labs in 1980. The invention of the HEMT represented the latest triumph of bandgap engineering and molecular beam epitaxy that had earlier brought to the world the heterostructure laser, the heterojunction bipolar transistor, heterostructure avalanche photodiodes and other electronic and photonic devices that would come to revolutionize communication systems. The HEMT was based on the concept of modulation doping first demonstrated by Dingle and collaborators at Bell Labs in 1978. A modulation-doped structure creates a two-dimensional electron gas at the interface between two semiconductors of different bandgaps. The spatial separation that is created between dopants and electrons confers these with a mobility that exceeds the bulk value even at relatively high carrier concentrations. The first demonstrations of modulation doping and the HEMT took place in the AlGaAs/GaAs system. These would not have been possible without the atomic layer precision growth capabilities of molecular beam epitaxy. Through MBE, heterostructures approaching monolayer-level abruptness, nearly perfectly coherent interfaces and precise dopant placement became possible. All these are essential ingredients for realizing modulation-doped structures with improved mobility over bulk values. The initial mobility enhancements that were observed were quite modest at

room temperature but much more significant at low temperatures. Over time, the low temperature mobility would dramatically improve leading to fundamental discoveries in solid state physics.

The first commercial application of a HEMT came from a totally unexpected area. In 1983 Fujitsu demonstrated a four-stage HEMT amplifier operating at 20 GHz. Its gain and noise performance was observed to improve significantly as the operating temperature was reduced. This was attributed to the improvement in mobility at low temperatures. These cryogenically cooled HEMTs significantly outperformed state-of-the-art GaAs MESFETs of the time. This result came to the attention of the Nobeyama Radio Observatory in Nagano (Japan) who ordered several low-noise amplifiers for their 45 m radio telescope. These were installed in 1985 and in 1986, this telescope discovered new interstellar molecules in the Taurus Molecular Cloud, about 400 light years away. The great stability of the HEMT, compared with the then conventional parametric amplifiers, allowed prolonged observations, something that had great value to astronomers. Since then, HEMTs have been widely used in radio telescopes throughout the world

The first mass-market applications of AlGaAs/GaAs HEMTs came in the communications arena after the recognition of their superior high-frequency noise characteristics over MESFETs. This was attributed to the excellent fT and the high aspect ratio of the channel. Direct Broadcasting Satellite receivers including low-noise HEMT amplifiers first went commercial in 1987. They enabled a reduction in antenna size by one half. By 1988, the yearly world-wide production of HEMT receivers was about 20 million [17].

II. 2.1. Background

In recent decades, novel semiconductor materials, such as GaN, metal oxides, and 2D materials, have been widely studied to further enhance the energy conversion and storage efficiency, owing to their superior material and device properties . Among them,

GaN-based AlGaN/GaN high electron mobility transistors (HEMTs) are good candidates for high power, high frequency, and low loss applications because of high critical breakdown field and high electron mobility. The breakdown voltage (BV) is one of the most important design targets, and the reported values are still far below the theoretical limit.

Therefore, it is of great importance to further improve the BV, especially not at the cost of increasing the device size. Several termination techniques have been proposed to improve the BV, such as field plate, fluorine ion implantation, and recessed gate-edge termination.

Fluorine ions implanted in the thin AlGaN barrier layer (FBL) has a simple fabrication process without inducing an additional parasitic capacitance; however, the peak position of the fluorine profile and vacancy distributions is near to the two-dimensional electron gas (2DEG) channel, which would inevitably cause significant static and dynamic characteristic degradation.

In order to better understand how an AlGaN / GaN HEMT works, we will describe the different strip structures of the materials constituting the latter. The juxtaposition of a material with a wide gap (AlGaN: 3.82eV), and another with a slightly more gap weak (GaN: 3.4eV), forms a heterojunction driven by the discontinuity of the conduction at the interface (ΔE_c). Figure 2.3 shows the energy levels of each material before contact. (Bernardini, 1997) [18].

II. 2.1.1. History of HEMTs

As many other discoveries, the idea for a HEMT structure was a product of a research with different purposes and there were several factors superimposed. The late 70s saw the evolution of the molecular beam epitaxy growth technique and modulation doping together with a vivid interest in the behavior of quantum well structures (the latter peaking in the work of Klitzing, Laughlin, Stomer, and Tsui).

At this time T. Mimura and his colleagues at Fujitsu were working on GaAs MESFETs.

Facing problems with a high-density of the surface states near the interface, they decided to use a modulation-doped heterojunction super lattice and were able to produce depletion type MOSFETs. While those structures were still plagued by several issues, the idea to control the electrons in the superlattice occurred to him. He achieved this by introducing a Schottky gate contact over a single heterojunction.

Thus, the AlGaAs/GaAs HEMT was born. Subsequently the first HEMT based integrated circuit was reported . Alongside Fujitsu a number of other research facilities joined on the further development of the new structures: Bell Labs, Thomson CSF, Honeywel, In order to counter different problems, several designs were proposed: AlGaAs/GaAs HEMTs, AlGaAs/InGaAs pseudomorphic HEMTs (pHEMTs), AlInAs/InGaAs/InP HEMTs (ordered by increasing). However, until the end of the decade HEMTs mainly found military and space applications . Only in the 90s the technology entered the consumer market in satellite receivers and emerging mobile phone systems. In the beginning of the last decade new methods for deposition of GaN on sapphire by MOCVD were developed. Thus, the production of AlGa_N/Ga_N-based HEMTs was possible . GaN has a wide band gap which brings the advantages of higher breakdown voltages and higher operational temperature. Due to the large lattice mismatch between AlN and GaN a strain in the AlGa_N layer is induced, which generates a piezoelectric field. Together with the large conduction band offset and the spontaneous polarization this leads to very high values for the electron sheet charge density. This large potential of AlGa_N/Ga_N structures (and the indirect advantage of excellent thermal conductivity of the sapphire substrates) was realized very soon and the research focus partially shifted from AlGaAs/GaAs to AlGa_N/Ga_N devices.

In the course of further development and optimization various techniques were adopted. An approach previously used in high-voltage p-n junctions , the field-plate electrode, significantly improved device performance by reducing the peak values of the electric field in the device. Thus, the breakdown voltage could be further increased.

This technique was further refined to T-shaped and subsequently Y-shaped gate electrodes . Another step in optimization of the structure is the addition of a thin AlN

barrier between the GaN channel and the AlGaN layer. It increases the conduction band offset and the two-dimensional electron gas (2DEG) density and decreases the alloy disorder scattering, thereby increasing the mobility. An additional option to enhance the electron gas transport properties is the double-heterojunction structure .

The InGaN layer under the channel introduces a negative polarization charge at the interface, and thereby improves the carrier confinement in the channel.

While the depletion mode (D-mode) technology has been significantly improved, no comparable progress on the enhancement counterparts can be noted. However, such devices have advantages in certain applications and are therefore getting in the focus of research activities in the recent years. Several groups have proposed interesting approaches. Devices featuring very thin AlGaN layers and Fluoride-based plasma treatment have been proposed, however certain stability concerns remain. A very promising method is the recess gate structure reported by Kumar et al. Also recently, excellent results have been achieved with InGaN-cap devices . [19].

II. 2.1.2. Working principle of HEMTs

HEMTs are essentially heterojunctions formed by semiconductors having dissimilar bandgaps. When a heterojunction is formed, the conduction band and valence band throughout the material must bend to form a continuous level. The wide band element has excess electrons in the conduction band as it is doped with donor atoms (or due to polarization charge in GaN-based HEMTs). The narrow band material has conduction band states with lower energy. Therefore, electrons will diffuse from wide bandgap material to the adjacent lower bandgap material as it has states with lower energy. Thus, a change in potential will occur due to movement of electrons and an electric field will be induced between the materials. The induced electric field will drift electrons back to the conduction band of the wide bandgap element. The drift and diffusion processes continue until they balance each other, creating a junction at equilibrium like a p-n junction. Note that the undoped narrow bandgap material now has excess majority charge carriers, which yield high switching speed. An interesting fact is that the low

bandgap undoped semiconductor has no donor atoms to cause scattering and thus ensures high mobility.

Another interesting aspect of HEMTs is that the band discontinuities across the conduction and valence bands can be engineered to control the type of carriers in and out of the device. This diffusion of carriers leads to the accumulation of electrons along the boundary of the two regions inside the narrow bandgap material. The accumulation of electrons can lead to a very high current in these devices. The accumulated electrons are also known as 2DEG. **Figure II.1** shows the generalized band diagram formed at the heterojunction for typical HEMTs. Both the conduction band (E_C) and valence band (E_V) bend with respect to the Fermi level (E_F) resulting in a quantum well filled with 2DEG and eventually, a conducting channel is formed. [20]

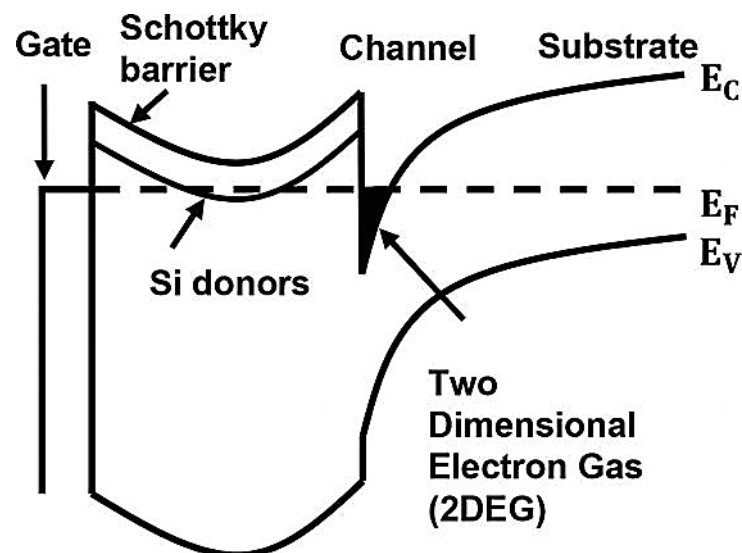


Figure II.1.Generalized energy band diagram of HEMTs[19]

II. 2.2. Al_xGa_{1-x}N/GaN HEMTs structure

Al_xGa_{1-x}N layers with high Al content which results in poor transport properties of Al_xGa_{1-x}N/GaN structures with $x > 0.5$. To overcome this problem, the ultra-thin all binary AlN/GaN material system, which can be grown reliably, has become an alternative candidate for future high-frequency power applications. Due to the large difference in spontaneous and piezoelectric polarizations between the GaN and AlN layers, the 2DEG which forms near the AlN/GaN interface can reach over $3 \times 10^{13} \text{ cm}^{-2}$ for an extremely thin AlN barrier layer thickness ($d < 5 \text{ nm}$) along with high mobility ($> 1000 \text{ cm}^2/\text{V}\cdot\text{s}$) and very low sheet resistance ($R_{sh} < 150 \Omega$). In addition, AlN with its relatively high dielectric constant and wide band gap (6.2 eV), provides better carrier confinement and has the potential to be an excellent choice for the gate dielectric. Compared to the AlGaN/GaN structure, the AlN/GaN structure offers a big reduction in alloy disorder scattering and roughness scattering (by removing Ga from the barrier). From a circuit design point of view, the use of very thin AlN barrier layer (3 - 5 nm) increases the intrinsic transconductance and decreases the short channel effects by placing the gate much closer to the 2DEG channel. Having these superior properties makes this material system have potentially the highest performance HEMTs in the III-V nitrides. In the early years, it was difficult to grow high quality material AlN/GaN heterostructures due to large lattice mismatch between AlN and GaN (2.4 %). A continuous surface-potential-based electro-thermal compact model suitable for the study of intermodulation distortion IMD in GaAs HEMT devices and a precise analytical calculation for the position of the Fermi level E_f in these devices from a consistent solution of Schrodinger's and Poisson's equations [20].

II. 2.2.1. GaN-based HEMTs

GaN-based HEMTs have the similar layered structure to conventional GaAs-based HEMTs as shown in Figure 5. But no intentional doping is required in AlGaN/GaN HEMTs. Rather electrons come from surface states due to the spontaneous polarization found in wurtzite-structured GaN. This accumulation of free carrier forms high carrier

concentration at the interface leads to a 2DEG channel. Figure 2 also indicates donor-like surface traps (empty) on top and thereby the positively polarized charge at AlGaN/GaN interface **Figure II.2**. The 2DEG is an explicit function of the surface barrier, AlGaN thickness and the bound positive charge at the interface. [21].

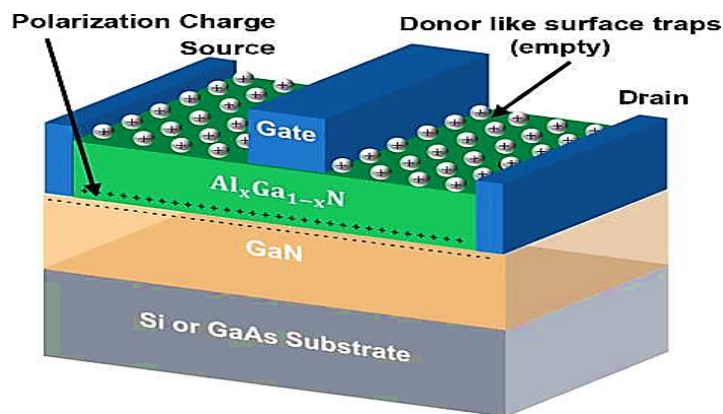


Figure II.2 .AlGaN/GaN HEMT structure[21]

II.2.2.2 Description of the structure of a HEMT

The structure of a gallium nitride HEMT transistor is very similar to that of a transistor whose semiconductor material is Gallium Arsenide despite several clear differences. We represent a typical structure of a HEMT AlGaN / GaN transistor by Figure II-5. It is made of the following materials:

- The substrate
- A material with a large gap
- A small gap material

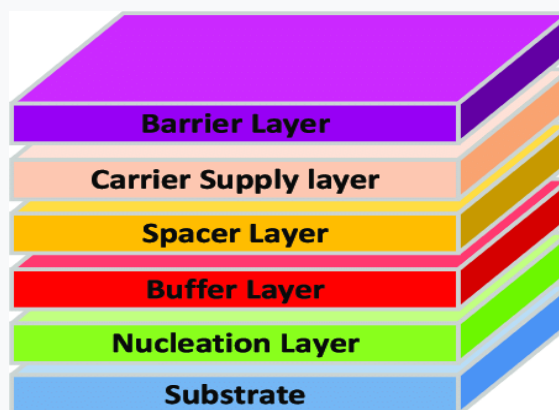


Figure II-5: Structure of a HEMT transistor

II.2 .2.3 Description of layers

- **Cap layer**

It is a surface layer, formed by a low bandgap material in order to achieve the ohmic source and drain contacts. This layer is in most cases strongly doped in order to reduce the value of the contact resistors and therefore that of the access resistors Schottky layer This non-doped large-gap layer makes the Schottky contact of the gate.

- **Donor layer**

As its name suggests, it supplies free electrons to the structure, the doping which is generally produced by a silicon doping plane, plays an important role there because it contributes to increasing the concentration of electrons supplied.

- **Spacer**

This layer of intentionally undoped wide-gap material allows the separation of electron donor atoms of the donor shell, electrons of the channel. The interactions electron-impurities are thus reduced, we notice that the thicker this layer, the better is the mobility of electrons in the channel on the other hand a thinner (thin) spacer favors a better electron transfer in the channel.

- **The channel**

This is the most important part of the HEMT, because it is in this place that the canal is created that receives the two-dimensional gas of electrons and it is this layer that will determine the performance of the component through the electron transport properties in the material.

- **The buffer layer**

In general, this layer has joint structural properties between that of the substrate and the channel material. It allows better growth of GaN, the type of face depends in part of this layer and it promotes the confinement of electrons by interposing the injection of carriers to the substrate.

• The substrate

This is the layer on which the epitaxial materials are grown. Its choice is crucial for the component quality and its functioning. Indeed, a bad choice of substrate can cause during the growth of dislocations, which can render the component non-functional. [22]

II.2.2.4. Formation and characteristics of 2DEG

The basic principle of a HEMT is the transfer of electrons from the donor atoms of the larger gap layer to the smaller gap layer to form the channel near the interface. The AlGaN / GaN HEMTs have a high charge density n_s from gas to electrons two-dimensional 2DEG that cannot be attributed solely to the large discontinuity of band between GaN and AlGaN but above all due to the presence of a strong hetero polarization interface.

The following figure shows an AlGaN / GaN HEMT, where the parameters d_d and d_i are respectively the thicknesses of the donor layer and the spacer

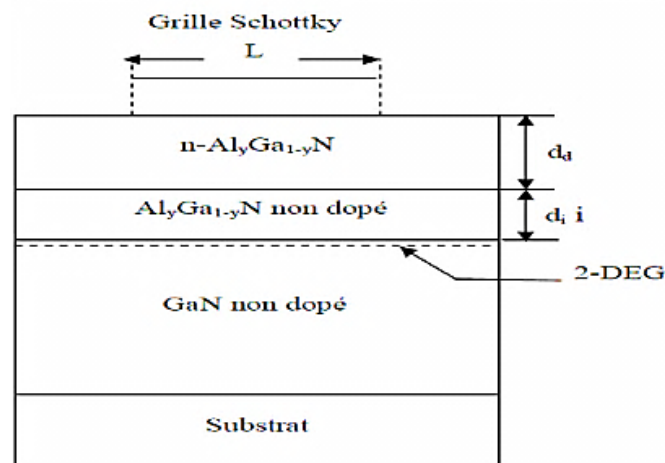


Figure II.6: Diagram of the AlGaN / GaN structure[22]

Due to the difference in the bandgap energies of the two materials, a well of potential is created at the interface, in which the electrons coming from the layer are confined donor and participant in the conduction current in the structure (figure I.9); this difference in

bandgap energies ΔE_g therefore influences the concentration of carriers and must be as large as possible.

Under the effect of polarization the bottom of the quantum well drops below the Fermi level, which in general is quite close to the middle of the bandgap of the material with the lowest gap [19]

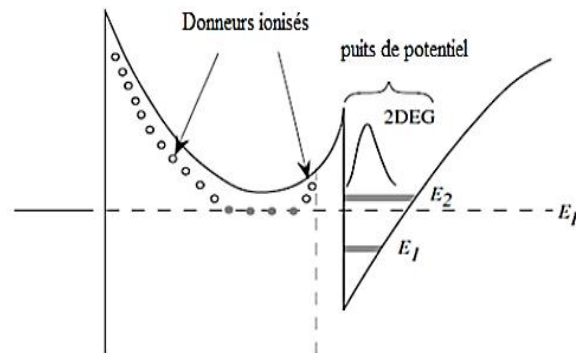


Figure II.7: Creation of a potential well in a HEMT transistor

II. 3. Growth techniques and substrates choice

II. 3.1. Silicon Carbide Substrates (SiC)

This substrate represents a perfect mesh agreement with GaN, as well as a good thermal conductivity $4.9 \text{ W}\cdot\text{cm}^{-1}\cdot\text{K}^{-1}$ comparing it to silicon, which gives it the possibility of dissipating heat well. However, its cost remains very high and the deposit of Gallium nitride on this substrate is very delicate. [23].

Silicon carbide SiC has a number of advantages over sapphire for GaN growing. First of all, the lattice mismatch for this pair is 3.1%. In addition, the thermal conductivity coefficient of SiC is high (3.8 Wt/cm K), whereas, doped SiC possesses high electrical conductivity. It implies that electric contacts can be mounted on the reverse side of a

substrate, and the technology of device manufacturing is sharply simplified here. There are both polar C-polar substrates of silicon carbide, the so-called C-substrates, and Si-polar substrates, i.e. Si substrates. In the first case, C-atoms go into the substrate surface, whereas in Si substrates just Si atom passes there. Nowadays, Si-substrates are more preferable, because GaN films grown on them are of top-quality. The main limitation of silicon carbide lies in its high cost. A high-quality 4 inch wafer costs about 3000 \$, whereas wafer of a larger diameter are not available now. Lattice mismatch of 3.1% leads to formation of defects in a marked quantity, and this fact opposes to develop high-current devices. In addition, after the termination of growth process, a need to etch off an initial substrate arises; C this is a hard task in the case of SiC, because etching off the material is a very tedious and complex process. Silicon carbide exists in more than 250 polytypes, which are characterized by alternation of various tightly-packed biatomic planes. The main element of all the polytypes is a covalent bonded tetrahedron formed of C-atoms and Si atom centrally located and vice versa a tetrahedron composed of Si-atoms with C-atom centrally positioned. [24]

II. 3.2. Sapphire Substrates

It is the most used for the manufacture of light emitting diodes and laser diodes. However, it has several major flaws. Indeed, the mesh disagreement with GaN is by 16% (after rotation of the epitaxial layer relative to the substrate) . dislocation densities of the order of 10^{10} cm^{-2} . However, with adequate nitriding and an optimized buffer layer deposited at low temperature, for example in AlN, very good quality GaN films with a dislocation density of less than $2 \times 10^9 \text{ cm}^{-2}$ can be obtained. On sapphire substrate, growth by MOVPE makes it possible to obtain GaN face-Ga type, while that by MBE allows to obtain GaN face-Ga or N-face. The disadvantages of sapphire are low thermal conductivity and great difficulty in being cut out. One of the cutting methods consists of making a groove with a laser, then engrave in this groove with a diamond saw, to finish by a cleavage .

Moreover, the substrate is in this case removed by "lift off" take-off and replaced by a substrate of higher thermal conductivity. Finally ; sapphire is an insulator, which does not allow an electrical contact to be directly placed on the substrate. Sapphire substrates are generally nitrided before the growth of GaN by a exposure of their heated surface, typically around 1073K (800 ° C), to a flow of ammonia.

It appears that an AlN monolayer forms during this step. An AlN buffer layer can optionally be deposited before growth. Note that this type of buffer layer is epitaxied at a temperature comparable to that of GaN growth and therefore differs buffer layers used in MOCVD. [25]

II. 3.3. GaN and AlN Substrates

Engineers at Fujitsu are claiming to have broken new ground for the performance of the RF GaN-based HEMTs operating in the X-band. Their device, made on an AlN substrate, delivers a power density of more than 15 W mm^{-1} , and far higher values could follow with the introduction of field plates and optimisation of device dimensions.

According to the team, the other reports of GaN-based HEMTs on AlN substrates have used AlGaN channels to improve higher-temperature performance. However, with that design alloy scattering in the ternary diminishes electron mobility and holds back performance. To avoid these issues, the team from Fujitsu employs a GaN channel.

Working with an AlN substrate promises to offer the best of both worlds, as this has a higher conductivity than GaN and avoids the lattice mismatch issues of SiC. But AlN substrates are pricey and limited in size.

Spokesman for the team, Shiro Ozaki, told Compound Semiconductor that he hopes that increased use of these devices for ultraviolet laser diodes and LEDs will help to address these issues. He expect that this will ultimately lead to the availability of affordable, 3-inch diameter substrates.

Ozaki and co-workers have produced a range of GaN HEMTs with a $0.25 \mu\text{m}$ gate length, a $50 \mu\text{m}$ gate width and a gate-to-drain length of $3 \mu\text{m}$. One of these transistors has been produced on a 1-inch diameter AlN substrate with a threading dislocation

density below 10^3 cm^{-2} , and another five variants have been fabricated on SiC: one, like that on AlN, has a channel thickness of 200 nm, to trim the drain-leakage current; and the other four have 1000 nm-thick channels and different AlGaN barrier compositions, to evaluate the impact of carrier density on DC characteristics.

Measurements of the drain current as a function of the drive voltage, which is the difference between the gate-to-source voltage and the threshold voltage, uncovered a leakage current

path for HEMTs that have a thick channel. Devices with the thinner, 200 nm-thick channel suppressed this leakage. The team also found that the AlGaN buffer with a high aluminium composition, employed in the device grown on the AlN substrate, sharply reduced the pinch-off state and had a lower leakage current than the similar device made on SiC.

To ensure excellent output power characteristics, HEMTs must produce a high drain current at a high blocking voltage. Measurements of the five devices made on SiC show that gains on one of these fronts are compromised by losses on the other, while the HEMT on AlN provides an unparalleled performance.

The team's GaN-on-AlN HEMT, which has a total gate width of 1 mm, produces a peak power-added efficiency of 49.1 percent when operating at 70 V, using 10 μs pulses at a 1 percent duty cycle. Associated output power is 41.7 dB, equivalent to 14.7 W mm⁻¹, and gain is 9.6 dBm.

For devices grown on SiC, a power density of 30.6 W mm⁻¹ has been reported in the X-band. "Our target is higher than that," says Ozaki.

To meet that goal, Ozaki and co-workers intend to increase the operating voltage for their HEMTs to more than 100 V. "To realise this, field plate optimisation will be a key technology." [26]

II .4.HEMTs operation

The high electron mobility transistor (HEMT) is a heterostructure field effect transistor. The term “HEMT” is applied to the device because the structure takes advantage of superior transport properties of electrons in a potential well of lightly doped semiconductor material. A simplified AlGaAs/GaAs HEMT structure is illustrated in **Figure II.3**

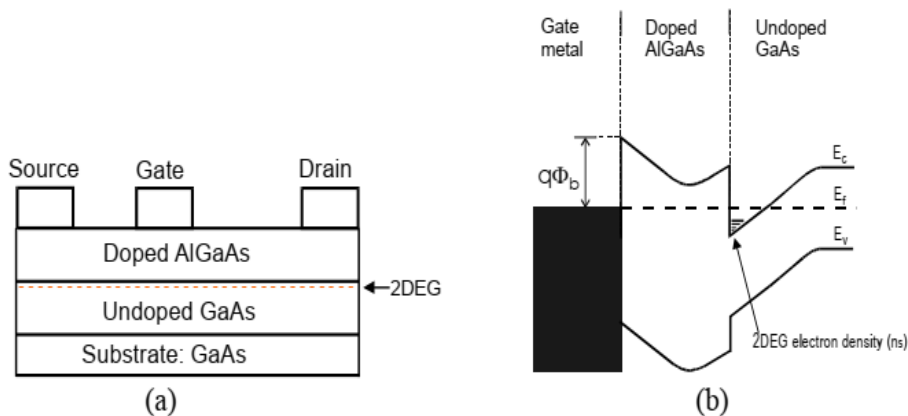


Figure II.3.(a) Simplified AlGaAs/GaAs HEMT structure, (b) corresponding band diagram.

As shown in the figure, a wide bandgap semiconductor material (doped AlGaAs) lies on a narrow band material (undoped GaAs). The band diagram of correlated structure is shown in **Figure 8.b**. A sharp dip in the conduction band edge occurs at the AlGaAs/GaAs interface. This results in high carrier concentration in a narrow region (quantum well) in source-drain direction. The distribution of electrons in the quantum well is essentially two-dimensional due to the very small thickness of the quantum well in comparison to the width and length of the channel. Therefore the charge density is termed a two dimensional electron gas (2DEG) and quantified in terms of sheet carrier density n_s . AlGaN/GaN HEMT has been fabricated in a similar way using doped or undoped AlGaN layer as shown in **Figure 8.a**. It has been observed that a 2DEG is formed in the AlGaN/GaN interface even when there is no intentional doping of AlGaN layer. It has also been observed that

when the AlGaN layer is intentionally doped, the charge density in the 2DEG is not proportional to the amount of doping. The fundamental question is, since there are no intentionally introduced atoms to supply electrons, what is the source of the electrons that form the 2DEG?

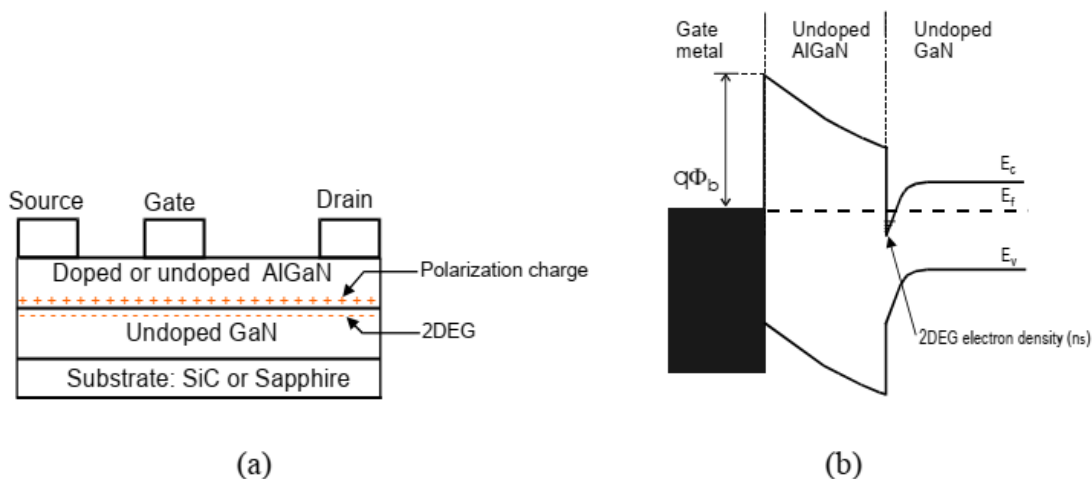


Figure II.4.(a) Simplified AlGaN/GaN HEMT structure, (b) corresponding band diagram.

In AlGaN/GaN HEMT, the formation mechanism of 2DEG at the heterointerface is different with that in the AlGaAs/GaAs HEMT. Due to the presence of a strong polarization field across the AlGaN/GaN heterojunction, a 2DEG with the sheet carrier density up to 10^{13} cm^{-2} can be achieved without any doping. Ibbetson et al. found that surface states act as a source of electrons in 2DEG. The built-in static electric field in the AlGaN layer induced by spontaneous and piezoelectric polarization greatly alters the band diagram and the electron distribution of the AlGaN/GaN heterostructure. Thus considerable number of electrons transfers from the surface states to the AlGaN/GaN heterointerface, leading to a 2DEG with high density. The band diagram of the structure shown in **Figure II.4. a** is illustrated in **Figure II.4.b** [27]

II .4.1.DC characteristics

Direct Current (DC) measurements are conducted to assess electrical properties of the fabricated devices. The measurement setup is composed of a semiconductor parameter analyser and a probe station. Schematic of the setup used in this work is provided in **Figure 10**. Probe station allowed easy addressing of small contacts.

and drain current is measured. This measurement is repeated at different gate bias. Important parameters to be measured are knee voltage (V_{knee}), pinch-off voltage ($V_{pinch\ off}$), maximum drain current (I_{ds}), transconductance (g_m) and breakdown voltage (V_{br}). A typical output IV curve of HEMT device is shown in **Figure 10**. The knee voltage signifies the voltage where saturation occurs in the graph. Also, maximum drain current is the intersection of the linear and saturation regions. Pinch-off voltage is where the drain current is almost zero. Transconductance is the ratio of the current change and is defined as

$$g_{m,DC} = \frac{\Delta I_{DS}}{\Delta V_{GS}} \mid V_{DC} = constant$$

Moreover, breakdown voltage is the maximum voltage that a device can handle when gate bias voltage is below pinch-off and drain voltage is increased until drain current reaches its maximum value I_{ds} . [14]

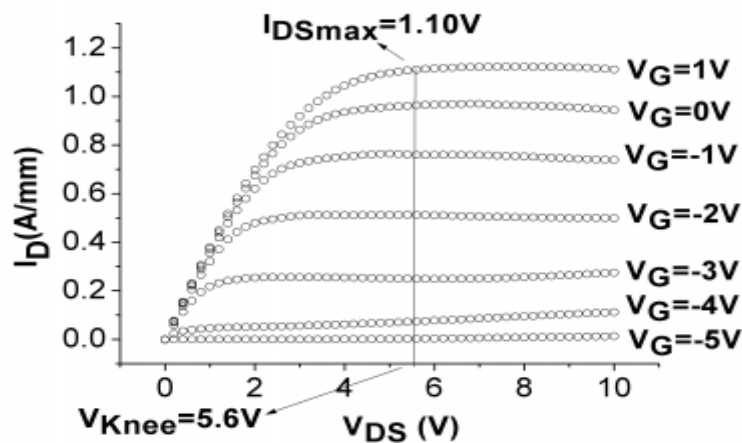


Figure II.5. A typical output characteristic of HEMT devices.

II .4.2.Degradation of HEMT performance

II .4.2.1.Degradation mechanisms

As the device design and material processing technology for AlGaN/GaN HEMTs has matured over the years, several failure mechanisms that limited device lifetime have been addressed and improved. These mechanisms can be grouped together into three main categories that affect lifetime: Contact degradation, hot electron effect, and inverse piezoelectric effect. Both Schottky and Ohmic contacts have shown excellent stability below 300 °C . Piazza et al. have reported an increase in contact resistance and passivation cracking due to Ga out-diffusion and Au inter-diffusion after a 100 h thermal storage test stress at 340 °C . Nickel based Schottky contacts have been shown to form nickel nitrides on GaN at annealing temperatures as low as 200 °C, resulting in a significant decrease in Schottky barrier height. [28]

The observed current collapse and gate lag in AlGaN/GaN HEMTs under high voltage and high current operation have been attributed to hot electrons. These are electrons that have been accelerated in a large electric field, resulting in very high kinetic energy, which can result in trap formation. Creation of traps can occur in both the AlGaN layer and the buffer, leading to reversible degradation of transconductance and saturated drain current . GaN is a piezoelectric material and under high bias conditions, the electric field induces additional tensile stress to the already strained AlGaN layer. Several authors have shown that upon reaching a “critical voltage”, irreversible damage to the device occurs resulting in defect formation through which electron leakage can occur Permanent device degradation after high VDG stress under on-state conditions has been attributed to the presence of hot electrons. In GaAs-based devices, hot electrons generate holes which are accumulated by the gate and result in a negative shift in V_T . Typically, IG is used to derive the field-acceleration laws for failure. Impact ionization, however, is negligible in GaN HEMTs. This is due to the fact that tunneling injection dominates gate current, preventing gate current from being used as an indicator for hot electron degradation . However, these hot electrons likely lead to trap generation at the

AlGaN/GaN interface and/or at the passivation GaN cap interface. As in GaAs and InP based HEMTs, traps lead to an increase in the depletion region between the gate and the drain, ultimately resulting in an increase in drain resistance and subsequently a decrease in saturated drain-source current. Comparatively, under reverse bias or so-called off-state conditions the degradation is greatly reduced due to the reduction of electrons present in the channel. Sozza *et al.* showed that GaN/AlGaN/GaN HEMTs that underwent a 3000 h on-state stress resulted in an increase in surface traps with an activation energy of about 0.55 eV. On the other hand, devices stressed under off-state conditions saw a very small increase in traps.

Meneghesso and *al.* have employed the use of electroluminescence (EL) to study the effect of hot-carriers and its dependence on stress conditions. Uniform EL emission was observed along the channel for devices stressed at $V_{GS} = 0$ V and $V_{DS} = 20$ V, which is due to hot electrons. However, there is no presence of hot spots or current crowding. On the other hand, under OFF state conditions with $V_{GS} = -6$ V and $V_{DS} = 20$ V (resulting in a $V_{GD} = -26$ V), the EL emission from the channel is not uniform. These hot spots may be due to injection of electrons from the gate into the channel. Due to the high bias conditions, the electrons acquire enough energy to give rise to photon emission. [29].

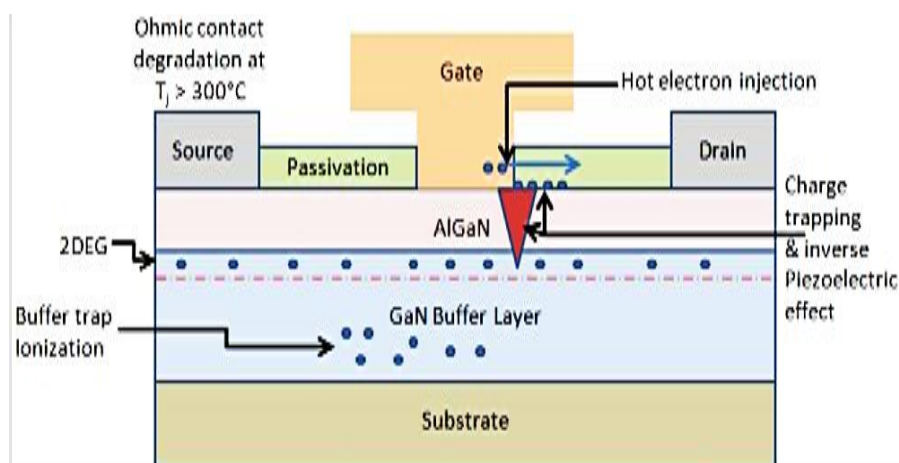


Figure II.5. Schematic of degradation mechanisms in AlGaN/GaN HEMTs.

II .4.3. Breakdown mechanisms Substrate

Thanks to the recent advancements in the growth and fabrication processes, the performance of high electron mobility transistors (HEMTs) based on GaN has significantly improved. The main advantages of using GaN as a material for the realization of HEMTs are the high sheet charge density ($>10^{13} \text{ cm}^{-2}$) of the two-dimensional electron gas (2DEG), which results in a low on-resistance of the transistors; the high thermal conductivity of GaN ($>2 \text{ W cm}^{-1} \text{ K}^{-1}$), which permits to reach high levels of power dissipation while keeping the channel temperature low; the high breakdown field (3.3 MV/cm), which allows to fabricate devices with breakdown voltages in the order of hundreds or thousands of volts, depending on gate–drain spacing and on buffer thickness. These unique features make GaN an almost perfect material for the manufacturing of high power transistors: thanks to the recent efforts of the scientific and industrial communities, GaN-based transistors with breakdown voltages in excess of 1.5–1.9 kV have been recently demonstrated, thus clearing the way for the adoption of HEMTs in power electronics. Moreover, thanks to the low (on-resistance) \times (device capacitance) product, GaN-based power HEMTs can reach high switching frequencies ($>40 \text{ MHz}$), and can therefore be used for the fabrication of high efficiency power conversion systems: converters with efficiencies in excess of 96–98% have already been demonstrated, thus proving the superiority of GaN with respect to more conventional semiconductors for power electronics.

Despite the high performance of GaN-based HEMTs, the lifetime of these devices can be shorter than expected, due to the existence of a number of physical mechanisms responsible for device degradation. Recent studies demonstrated that GaN HEMTs may degrade due to the following processes:

(a) degradation of the gate Schottky junction, induced by off-state stress. This mechanism induces an increase in the gate leakage current, due to the generation of

localized shunt paths in proximity of the gate edge.

(b) semi-permanent or permanent degradation due to hot electrons. this mechanism occurs when the devices are operated in the on-state, and — in most of the cases — results in a decrease in drain current, due to the accumulation of negative charge close to the gate edge and/or in the gate–drain access region.

(c) delamination of the passivation, due to the exposure to high temperature/power levels, which may result in additional charge trapping and leakage processes.

(d) time-dependent degradation processes, due to the generation of defects within the AlGaN/GaN heterostructure. Besides these mechanisms, power devices operated at high drain voltages may show important breakdown (BD) processes. breakdown consists in a rapid increase in drain current, which occurs — in the off-state — when the drain voltage reaches a critical value. Breakdown may be catastrophic (i.e., induce a sudden failure of the devices); this typically happens when BD measurements are carried out in voltage controlled mode, by increasing the drain voltage until a un-controllable increase in drain current is triggered. A sustainable breakdown condition can be reached if the measurements are carried out in current-controlled mode: by using this method it is possible to separately evaluate the contribution of gate, source, and bulk leakage to the overall BD current, thus extracting information on the physical origin of breakdown for several operating conditions.

- The presence of relatively high breakdown current components at the gate, which can be either related to the leakage through the Schottky junction, or to surface-related conduction.
- Vertical breakdown, which can be due to a poor compensation of the buffer, to the use of a conductive substrate, and can be limited by the adoption of suitable back barrier or heterostructure configurations.
- Impact ionization mechanisms, that may induce a significant increase in drain current due to the generation of electron–hole pairs close to the gate. [30]

II. 5 Summary

In this chapter we have described the structure and the operation HEMTs transistors in particular HEMT's DC characteristics using an ALGAN / INGAN / GAN structure under the effect of the parameters specifies the constituent material the heterostructure and the dimensions of the transistor in order to optimize the performance of the transistor.

The increase in the current provided by the increase of NS and also responsible for The future HEMT devices based on two-dimensional carrier confinement seem very bright in electronics, communications, physics, and other disciplines. GaAs, InP, and GaN-based HEMTs will continue their journey toward higher integration, higher frequency, higher power, higher efficiency, lower noise, and lower cost. GaN, in particular, offers high-power, high-frequency territory of vacuum tubes and leads to lighter, more efficient, and more reliable communication systems.

HEMTs will continue to mold themselves into other kinds of FETs that will exploit the unique properties of 2DEG in various materials systems. In power electronics, GaNbased HEMTs can create a great impact on consumer, industrial, transportation, communication.

.Operating voltage reduction may be a solution to meet this challenge. Quantum well based devices such as InGaAs or InAs HEMTs offer very high potential.

Therefore, HEMTs may extend the Moore's law for several more years which will be gigantic for the society . it can be anticipated that, researching on new device models and structures of HEMTs will definitely result in new insights into the often bizarre physics of quantized electrons.

CHAPTER III

Simulation results and discussion

III-1. Introduction.

In recent years, due to the high costs of experiments, The researchers turned to simulation. It is widely used in the field letter and allows setting the most important parameters for the right Machine operation, reduce losses and improve parameters The physical and engineering of these devices In the first part of this chapter we will present the definition of which simulation tool to use. To modify our HEMTs. In the first part of this chapter we will present the definition of which simulation tool to use.

To modify our HEMTs.

We use SILVACO-TCAD software. TCAD is an acronym Computer Aided Design Technology. This is a computer aided design toolIt allows in our case to simulate the structure of HEMTs (doping, nature of materials, engineering ...). TCAD So it helps in designing components and/or understanding mechanisms the quantitative precision of the simulations depends on the fineness of the mesh that is applies to the structure. However, the calculation time of these simulations is proportional to the number of nodes composing the mesh. The limits of TCAD simulations are therefore linked to the mesh as well as to the approximations induced by the models used. SILVACO offers a wide choice of pre-implemented models; unfortunately these were developed primarily for silicon and gallium arsenide. So it is necessary adapt these models and to choose them correctly for gallium nitride (GaN) and Gallium aluminum nitride ($\text{Al}_x\text{Ga}_{(1-x)}\text{N}$) used in our device. Like the solving the equations, is carried out by Newton's method; convergence and therefore the resolution of our equations, is greatly complicated with an enlargement of the mesh .

The $\text{Al}_x\text{Ga}_{(1-x)}\text{N}$ and GaN hetero-structures have attracted wide attention for their high power and high frequency capability even under difficult conditions (from temperatures or high drain voltage). Recently $\text{Al}_x\text{Ga}_{(1-x)}\text{N} / \text{GaN}$ on substrates semi-insulators have been reported with high power efficiency and high power at the K band .

So these physical properties make it possible to realize HEMTs transistors with drain current densities greater than 1.4 (A / mm), high cutoff frequencies around 100 GHz and breakdown source voltages of around 100V. Simulation is a very important means for understanding and explaining certain physical phenomena which govern the functioning of the devices electronics and their performance, this chapter is devoted to the simulation and the interpretation of the simulation results obtained [31]

III.2 About the simulation software

SILVACO (Silicon Valley Corporation) is a software that allows to design, model and simulate the performance of semiconductor devices, before manufacturing prototypes testing. It is very useful in research and development projects because it optimizes the time of testing and therefore reduces the cost of designing and manufacturing devices electronic.

The TCAD-SILVACO includes new physical models that use methods and efficient numerical algorithms, new meshing techniques, linear solutions optimization, etc., while making it possible to obtain simulation results very close to those of practice. The major advantage of this type of simulator is to visualize in space the physical phenomena that are difficult to access and observe and to appropriate educational manufacturing processes. TCADSILVACO modules can be used for: Simulation of technological manufacturing steps (ATHENA, SSupreme3, etc.).[32]

III.2.1 ATLAS simulation tools (from the company SILVACO)

ATLAS simulation software is a modeling simulator two-dimensional components, it allows the resolution of differential equations derived from the physics of components such as those of diffusion or transport for discrete geometries it is therefore able to predict the electrical characteristics of the Most semiconductor components in continuous, transient or frequency mode. In more "external" electrical behavior. ATLAS

has been designed so that you can use other tools that facilitate its use, these tools are as follows [33]

1-DEVEDIT

Environment where the structures of the devices are drawn (dimension, doping, ...) and its mesh, It can be used to produce a new mesh on an existing structure, to modify a device or to create a device from scratch.

These devices can then be used by the 2D and 3D simulators from SILVACO.

2-DECKBUILD

Environment where the results of the simulations are displayed (structure of the component, distributions of various sizes in it, characteristics electrical ...). Tonyplot is therefore designed to visualize 1D and 2D structures produced by SILVACO simulators, It also provides many specific functions TCAD visualization such as 1D section lines, animation of markers to expose the variation of the vectors, integration of the 1D data files or the files (.log). There is also another tool similar to this one, except that it is designed to visualize 3D structures, named TonyPlot3D.

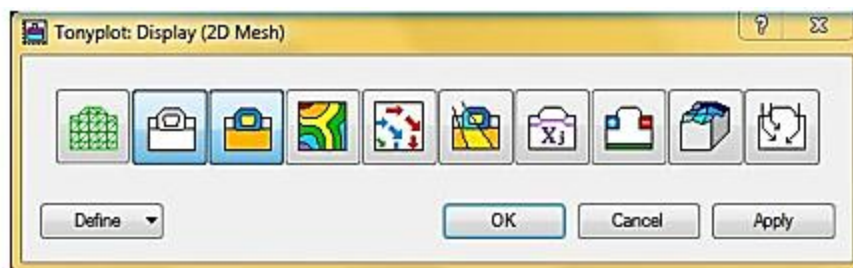


Figure III-1: the Tonyplot environment,

3-Optimize

Optimizes the parameters of the structure so as to finally obtain the value of parameter that we have defined beforehand. This tool therefore allows optimization for the calibration of trial and device simulators. It therefore makes it possible to adjust automatically the electrical parameters or the parameters of the process by playing on a or more input parameters

III.2.2 The Mesh:

Mesh plays an important role in obtaining good simulations. This one must be done with the greatest care to ensure the reliability of the results. The part mesh is a series of definitions of horizontal and vertical lines as well as the spacing between them, this spacing must be chosen according to the dimensions of the parts of our device . The precision of the simulation depends on the condition of the mesh. A thick mesh produces a quick simulation, but the results are less precise. While a fine mesh produces a slower simulation, but more precise results. So the mesh end is more interesting from a result point of view in the simulation

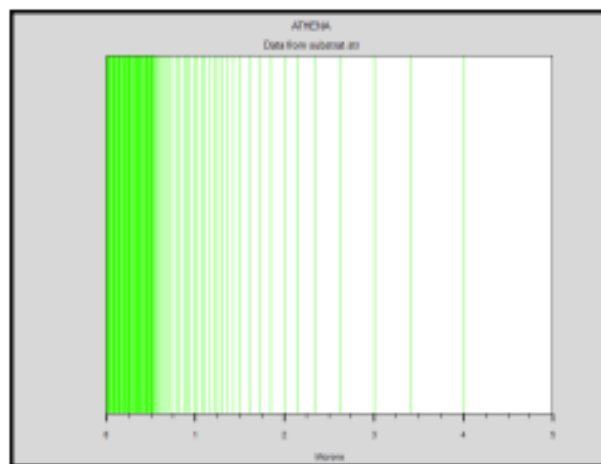


Figure III-2; mesh definition

III.2.3 The substrate and the doping:

The initial step is the definition of the starting substrate, i.e. the material on which will make our device so will choose the most used silicon substrate single crystal orientation = $\langle 100 \rangle$. which ensures better gate oxide quality, and then doped our material with phosphorus to have a N substrate (Figure III-3) (Figure III-3). [34]

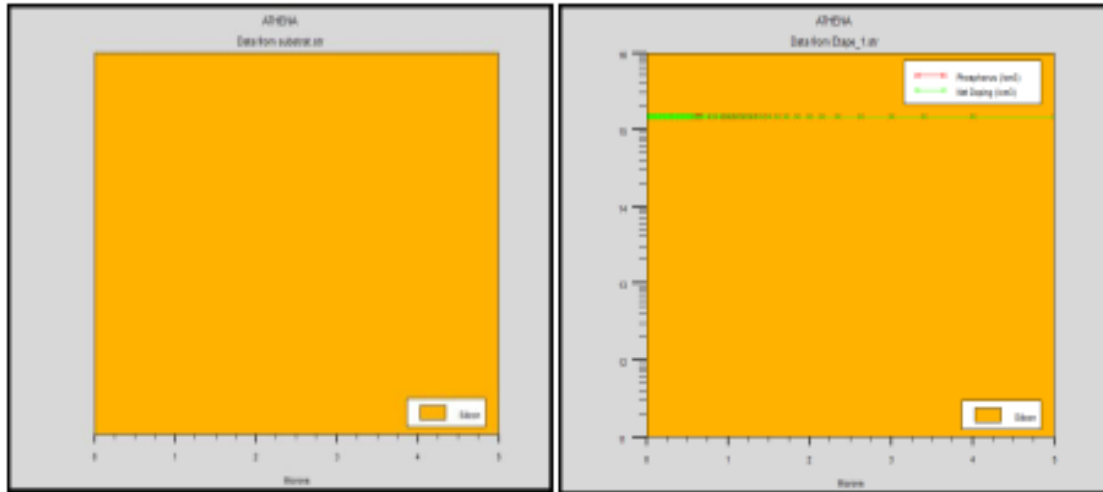


Figure III-3: definition of the substrate Figure III-3: doping of phosphorus

III 2.4. The programming steps:

After the presentation of the internal composition of SILVACO-Tcad software we will now present the order of the commands to the Atlas programming logic.

there are five groups of commands, these groups must be correct. if the order is not respect, an error message appears and the program is not executed in one way correct .

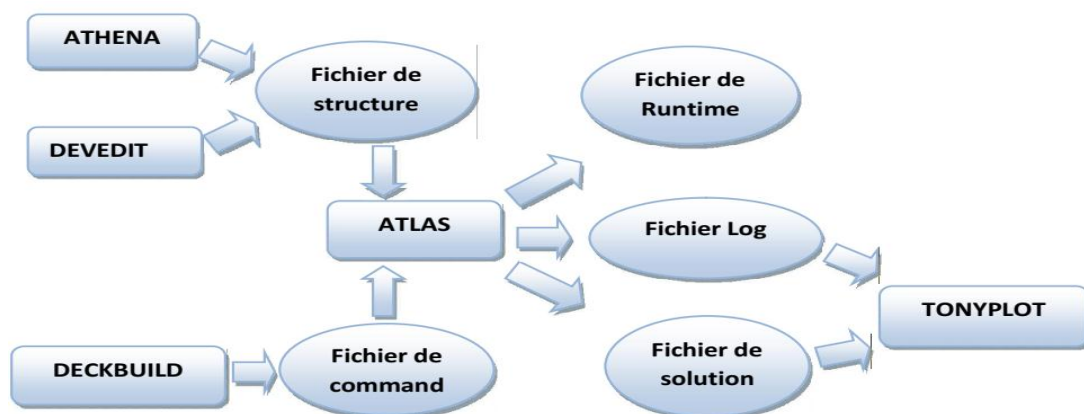


Figure III.4 ATLAS entrances and exits

III.3 Physical Models for Current in AlGa_N/Ga_N HEMTs

Since the use of wide bandgap materials for FETs has flourished, GaN-based HEMTs have demonstrated to be one of the best devices for high power and high frequency applications. Accurate modeling of these devices is therefore critical in high power RF circuit design. In this paper, compact physics-based models are desirable since they are relatively stable, use few parameters and can be used for almost all the operating modes of the device. However, the fact that most physical models are computationally complex and time consuming restricts their application in circuit simulations. A model based on device physics but still simple enough would be an ideal tool to use. Most of the existing HEMT physical models rely on an accurate description of the 2-DEG at the heterostructure junction. Due to the various energy levels and Fermi potential positions that need to be considered while calculating the charge in the region, the charge and current models often end up being complex and unattractive for circuit design. In this paper, we present simple physics-based models for the $C-V$ and $I-V$ characteristics of AlGa_N/Ga_N HEMT devices based on calculation of the electron density in the

TABLE III . 1 liste of symbols

symbol	Description
q	The electroncharge
V_{th}	Thermal Voltage
ε	The dielectric of AlGa _N
d	Thickness of AlGa _N layer
E_f	Position of the Fermi level
E_0	Position of the first energy level in the quantum well
E_1	Position of the second energy level in the quantum well
D	Density of electron
γ_0, γ_1	Parameters determined from experiment
n_s	Density of electron in 2DEG
C_g	Gate Capacitance per unit area (ε/d)

Channel region. The models assume that a good accuracy can be obtained by considering only one energy level in the triangular approximation of the quantum well created at the AlGa_xN/GaN interface. The model described in [1] was developed based on a similar assumption where the expressions for the above and below threshold regions were developed separately and the charge sheet approximation was assumed. This has made the total current model quite complex. The C - V and I - V models we present are developed from a simple unified charge control model, derived from the AlGa_xN/GaN quantum well-band structure and is valid for the whole range of operating regimes, which resulted in continuous compact charge and current models. Other than being simpler than the model in [1], our new model is more physical since it does not assume the charge sheet approximation. The derivation of the core current model is presented in Section II-A. Incorporation of additional effects into the core model is presented in the consecutive sections. Section III discusses the charge and capacitance models. In Section IV, results obtained using the models are shown compared with measurements and discussed. Finally, the conclusions are drawn in Section V

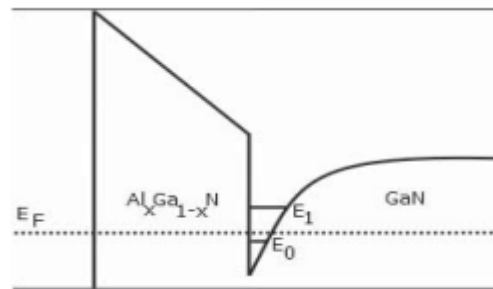


FIGURE. III.5Heterostructure interface and energy band profile of an AlGa_xN/GaNHEMT.

III.3.1 ANALYTICAL CURRENT MODEL

The basis of the analytical current model and its complete description is given in this section. The discussions of important effects such as channel length modulation (CLM) and short channel effects (SCEs) follow subsequently.

a- Core Current Model

In heterostructures such as AlGa_N/Ga_N and AlGaAs/GaAs the charge density per unit area accumulated in the potential well at the interface can be calculated with the assumption of a quasi-constant electric field in the potential well (triangular well approximation) and two subbands as

$$n_s = DV_{th} \left[\ln \left(e^{\frac{E_f - E_0}{V_{th}}} + 1 \right) + \ln \left(e^{\frac{E_f - E_0}{V_{th}}} + 1 \right) \right] \quad (1)$$

These subbands are given by

$$E_0 = \gamma_0 n_s^{2/3} \text{ and } E_1 = \gamma_1 n_s^{2/3} \quad (2)$$

where γ_0 and γ_1 are constants estimated from Shubnikov De Hass or cyclotron resonance experiments (all other symbols have standard definition as given in **Table III. 1**). When the gate depletion and channel depletion overlap to give a fully depleted barrier layer, the carrier density is given by

$$ns = \frac{\epsilon}{\rho d} (V_{g0} - E_f) \quad (3)$$

where $V_{g0} = V_g - V_{OFF}$, where V_{OFF} is the cutoff voltage. In the triangular quantum well created at the interface of AlGa_N/Ga_N, the second energy level is much higher than the first one and is well above the Fermi level for the whole operating range of the gate voltage. Thus, here the contribution of only the first energy level is considered. Therefore, (1) can be approximated as

$$ns = DV_{th} \ln \left(\exp \left(\frac{E_f - E_0}{V_{th}} \right) - 1 \right) \quad (4)$$

The expressions of E_0 and E_f from (2) and (3), respectively, can be used in (4) to establish a correlation between V_{g0} and ns given as

$$V_{g0} = \frac{qdn_s}{\epsilon} + \gamma_0 n_s^{2/3} + V_{th} \ln \left[\exp \left(\frac{n_s}{DV_{th}} \right) - 1 \right] \quad 5$$

The exponential term in (5) can be expanded into a Taylor series and the first few terms can be used. The first term gives a good approximation. In addition, (5) can be extended to any channel point by considering V as the local quasi-Fermi potential. Therefore, we have

$$V_{g0-V} = \frac{qdn_s}{\epsilon} + \gamma_0 n_s^{2/3} + V_{th} \ln \left(\frac{n_s}{DV_{th}} \right) \quad (06)$$

An analytical current model can be formulated using the definition of the drain current along the channel given as

$$I_{ds} = W\mu qn_s, \text{ or } I_{ds} = \frac{W}{L} \int_{V_1}^{V_d} qn_s \mu dV \quad (7)$$

where W is the width, L is the channel length, μ is the low field mobility of the device, and V_d and V_s are the drain and source voltages, respectively. dV with respect to the charge density obtained from the derivative of (6), which enables integration over the charge density, can be given as

$$dV = \left(\frac{qd}{\epsilon} + \frac{2}{3} \gamma_0 n_s^{-1/3} + V_{th} n_s^{-1} \right) dn_s \quad (8)$$

Using (8) in (7) and integrating from source to drain will give a simple analytical model of the drain current, which can be written as

$$I_{ds} = -\frac{q\mu W}{L} \left[\frac{qd}{2s} (n_D^2 - n_S^2) + \frac{2}{5} \gamma_0 \left(n_D^{5/3} - n_S^{5/3} \right) + V_{th} (n_D + n_S) \right] \quad (9)$$

where n_s and n_d are the charge carrier concentrations at the source and drain, respectively, and d is the barrier layer thickness and all the other symbols have the standard definition. The current model in (9) can satisfactorily be used to reproduce the I - V characteristics of a long channel device. n_s and n_d can be obtained iteratively from (6). Anyway, sufficiently accurate explicit expressions would make the model computationally faster.[35]

b-Surface potential

The fermi level is calculated using , which is valid in all regions of operation

$$E_{f,unified} = V_{go} - \frac{2V_t \ln(1 + e^{\frac{V_{go}}{2V_t}})}{\frac{1}{H(V_{go,p})} + (C_g/qD)e^{-\frac{V_{go}}{2V_t}}} \quad (10)$$

where, $V_{go} = V_{gs} - V_{OFF}$, V_t is the thermal voltage, C_g is the gate capacitance per unit area, q is the electronic charge and D is the density of states. $V_{go;p}$ is equal to V_{go} for gate voltages above the threshold voltage and is of the order of thermal voltage in the sub-threshold region. This fermi level is then used in the calculation of the surface potential , at both ends of the channel

c- Charges

The surface potential calculated at the source and drain ends of the channel (s and d respectively) is used to calculate the intrinsic charges, using the Ward-Dutton partitioning scheme as

$$Q_g = - \int_0^L qWC_g(V_{go} - \psi)dx \quad (11)$$

$$Q_d = - \int_0^L \frac{X}{L} qWC_g(V_{go} - \psi)dx \quad (12)$$

$$Q_g = -Q_g - Q_s \quad (13)$$

d. Drain current

The core drain current model, including mobility degradation and velocity saturation, is given as

$$I_{ds} = \frac{\mu_{eff} C_g}{\sqrt{1 + \theta_{sat}^2 \psi_{ds}^2}} \frac{W}{L} (V_{go} - \psi_m + V_{th}) (\psi_{ds}) (1 + \lambda V_{ds,eff}) \quad (14)$$

where L and W are the gate length and width respectively, λ is the channel length modulation parameter, μ_{eff} is the effective mobility considering the degradation due to vertical field, and θ_{sat} is the velocity saturation parameter. Also $m = d+2s$ and $ds = d - s$.

e-Access region resistance

The total source and drain access region resistance is given by where $R_{sc(dc)}$ is the contact resistance .

$$R_{S(d)} = \frac{R_{sc(dc)}}{W} + R_{s0(d0)/(R0)} [1 - (I_{ds} / I_{sat,accs})^M]^{1/M} \quad (15)$$

f- Gate current

The current density corresponding to the Poole-Frenkel (J_{PF}) part of the gate current is given as

$$J_{PF} = C.E. \exp(\alpha + \beta\sqrt{E}) \quad (16)$$

ηV where α and β are material dependent constants. Using $E = \frac{q\sigma_p - C_g(V_{go} - \psi)}{\epsilon}$, where σ_p is the effective polarization charge, we can get the current as $I_{PF} = W R_0 L J_{PF} dx$. Similarly, the Thermionic emission and Trap assisted tunneling parts can be calculated using their corresponding current densities (J_{TE} and J_{TAT} respectively) given as [36]

$$J_{PF} = J_{TE0} [\exp\left(\frac{V}{\eta V}\right) - 1] \quad (17)$$

$$J_{TAT} = J_{TAT0} \left[\exp \left(\frac{V - V_0}{\eta_2 V_t} \right) \right] \quad (18)$$

III.4 HEMT device structure

It is a question of defining the most realistic structure. The construction of the structure consists of four steps: definition of the mesh, definition of the regions, definition of the electrodes and definition of doping, according to

a-MESH (mesh definition): The mesh divides the simulated structure into small cells to be able to solve the fundamental equations numerically. The mesh element used is the triangle. To ensure good precision during simulation, it is necessary to have the mesh as fine as possible. On the other hand if the mesh is very fine, the computation time is very high because there are more items to calculate. The general format to define the mesh is

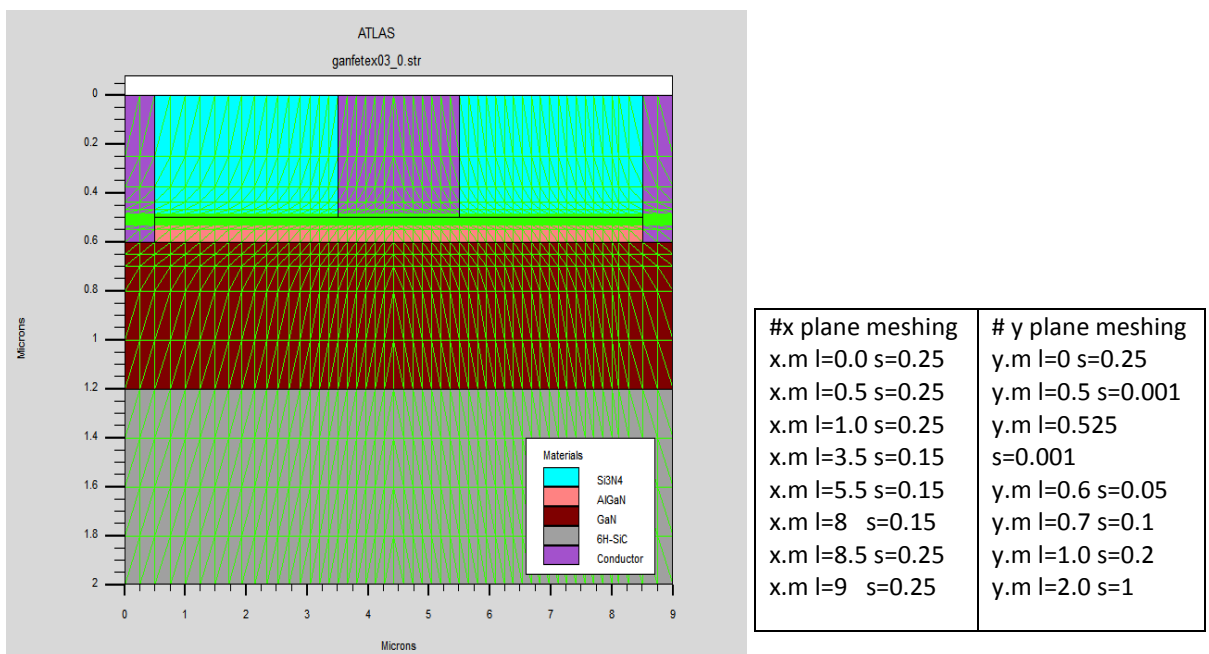


Figure II.5: Mesh of our structure

b-REGION (definition of regions): After having defined the mesh, it is necessary to define regions for which the format for defining regions with dimensions in micrometers is the following :

```

region num=1 x.min=0 x.max=9 y.min=0.0 y.max=0.5 mat=nitride insulator
region num=2 x.min=0 x.max=9 y.min=0.500 y.max=0.600 mat=AlGaIn x.comp=0.3
region num=3 x.min=0 x.max=9 y.min=0.6 y.max=1.2 mat=GaIn
region num=4 x.min=0 x.max=9 y.min=1.2 y.max=2 mat=SiC substrate
  
```

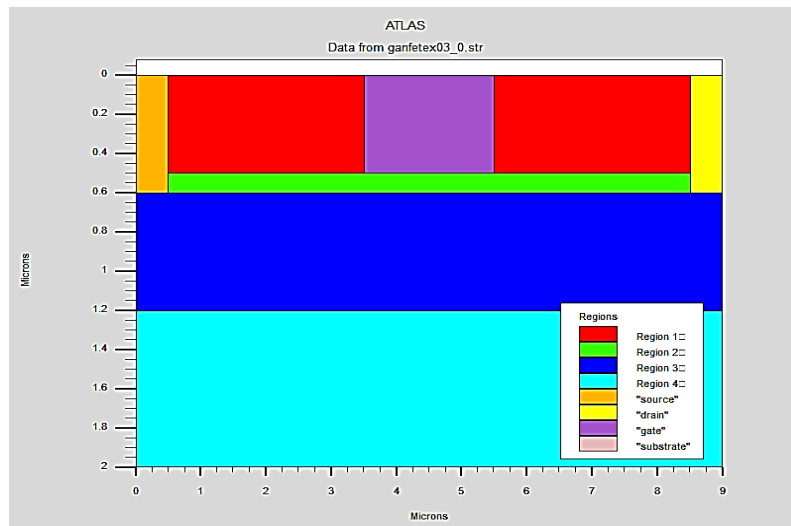


Figure III.6: Regions of our structure

c-LECTRODE: Atlas has a limit of 50 electrodes that can be set. definition of electrodes is as follows: ELECTRODE name = <electrode name> <parameter position>

```

elec num=1 name=source x.min=0 x.max=0.5 y.min=0 y.max=0.6
elec num=2 name=drain x.min=8.5 x.max=9 y.min=0 y.max=0.6
elec num=3 name=gate x.min=3.5 x.max=5.5 y.min=0 y.max=0.5
elec num=4 substrate
  
```

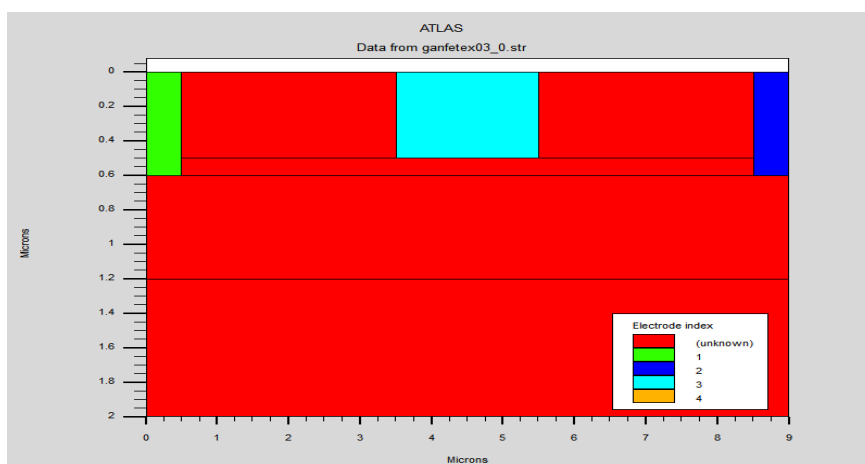


Figure III.7: Electrodes of our structure

d-DOPING (definition of doping): The last aspect of the construction of the structure is doping. The doping can be n or p type, also the distribution can be uniform, Gaussian, ... etc ,The format of the doping declaration in ATLAS is as follows

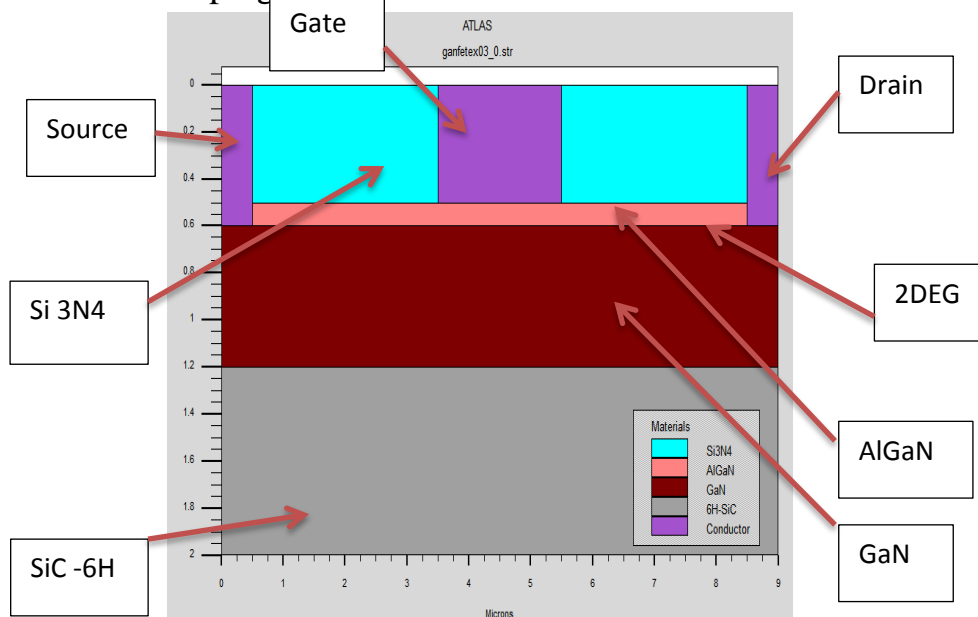


Figure III.8 The structure of HEMT $\text{Al}_{0.30}\text{Ga}_{0.70}\text{N} / \text{GaN}$ simulated by Atlas-Silvaco, on the left the Representation of the different regions and on the right the representation is made according to the type of material.

III.5 IV characteristics

HEMT, although different to a conventional MOSFET in terms of operation, is still a field effect transistor. Thus as a transistor it was developed in order to control large currents using small driving signals. HEMTs have a high potential especially in the high power and high frequency applications. To characterise the DC properties of a transistor a series of graphs is used, among which the I-V (current-voltage) characteristics called output and transfer characteristics are most known.

HEMT primarily works in depletion mode, i.e. current flows through the device even with no gate drive voltage. Voltage which has to be applied on the gate electrode in order to stop the current flow is called the pinch off voltage V_p . The best way to understand the HEMT electrical behavior is to develop a theoretical model and simulate the I-V characteristics. Figure III.8 shows the cross-sectional view of an AlGaN/GaN HEMT used for the simulation. The layer sequence is, from top to bottom,

metal/n-AlGa_N/undoped-AlGa_N/undoped-GaN with a 2-DEG formed at the unintentionally doped (UID)-AlGa_N/GaN interface. Figure III.9 shows the output Current-Voltage characteristics for different gate voltage V_{gs} ranging from -3 V to 0 V where -3 V is pinch off voltage V_p .

III .6. Results and discution

III.6.1 Description of the simulated structure

The topology of the studied structure is that of a HEMT Al_{0.30}Ga_{0.70}N / GaN epitaxy on a substrate (SiC-6H). The substrate size is $7.2 \mu\text{m}$,Number of boundary nodes= 53 Epitaxy consists of a layer of AlGa_N $0.9\mu\text{m}$, followed by $5.4 \mu\text{m}$ of a layer of GaN will contain in its area upper, the two-dimensional gas (2DEG) or electron channel. Source, gate and drain contact lengths are $0.3\mu\text{m} / 1\mu\text{m} / 0.3\mu\text{m}$

respectively. Source-to-gate and gate-to-drain distances are $2\mu\text{m}$, $3\mu\text{m}$. The charge density at the interface Al_{0.3}Ga_{0.7}N / GaN is fixed at $0.99 \times 10^{13} \text{cm}^{-2}$. The Schottky contact is given by the function of WF work (work function) equal to source 3.93eV , drain 3.93eV ,gate 5eV

model polarization calc.strain polar.scale=0.8 ,band gap to appear as the conduction band discontinuity

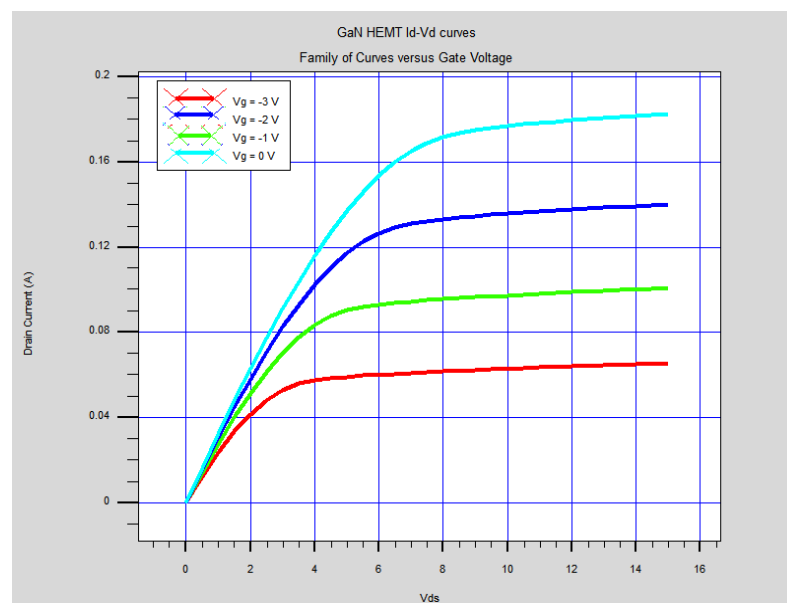


Figure III.9: The drain current-drain voltage characteristics for gate voltages

$V_g = -3, -2, -1, 0$ Volt

We notice in reading the curve that at 0, the current is large, and the lower it is, the current will be low for the conductor. The curve in red indicates the current surge towards the drain linear regime (the current I_{ds} increases with the voltage V_g):

If $V_g < V_d$.

$-V_g$ Voltage gate

$-V_d$ Voltage drain

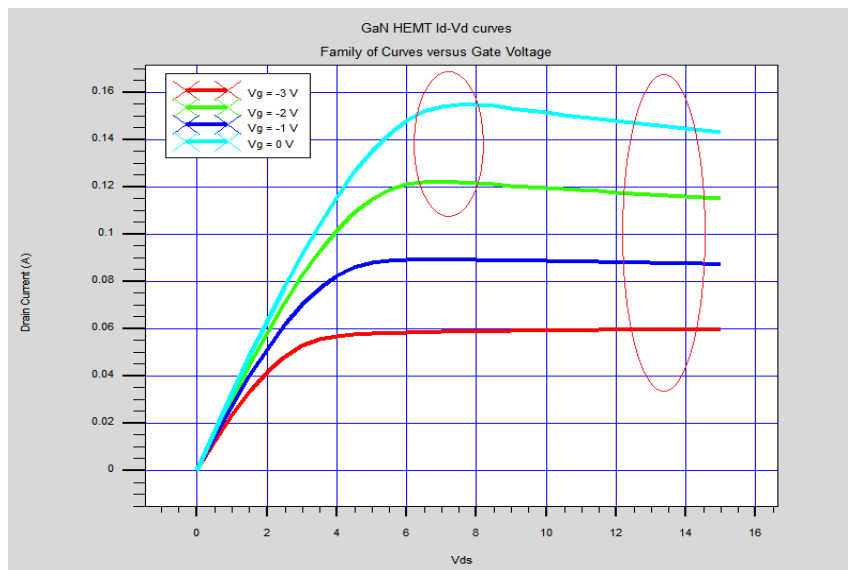


Figure III 10: The output drop return point (V_{ds}) of a HEMT transistor

Note of the Modes Operation, linear system for low values of drain source voltage V_{ds} and Saturation regime for high values, we also see a breakdown that appears slightly at values 08 and 15 V_{ds} values, , due to self-heating which is a major criterion limiting the performance of the transistor HEMT under electric polarization. Indeed, the charge densities being very high beyond eight volts in V_{ds} , the $I_{ds}(V_{ds})$ characteristics in continuous mode, present a decrease due to the degradation of the transport properties (the square resistance increases and mobility drops drastically) following a rise in temperature in the canal. This temperature rise is achieved in transistor operation, at the output of the grid on the drain side and is therefore often accompanied by a grid breakdown, note that the choice of the substrate and the passivation layer are then fundamental to best dissipate this heat

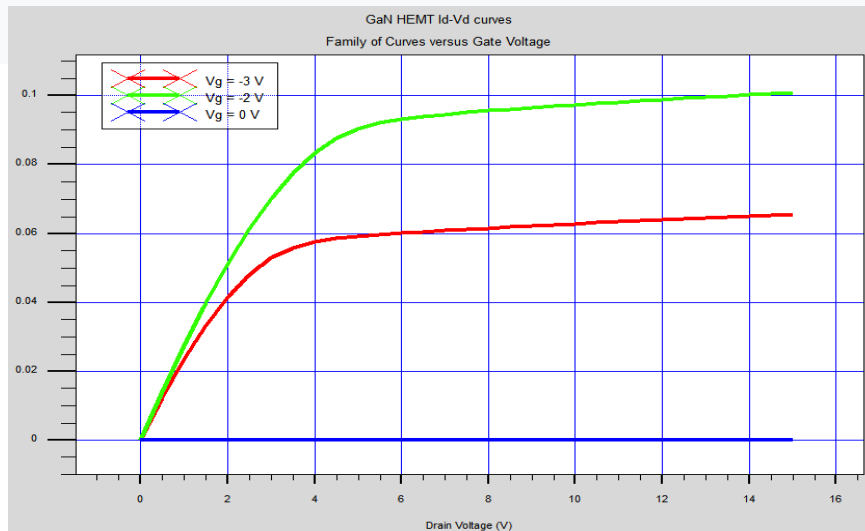


Figure III.11: Evolution of the network temperature in the component for $V_{gs} = 0$ and -2 V Influence of the substrate (a) 4H-SiC, I_{ds} - V_{ds} output characteristics for $V_{gs} = 0$ and -2 V.

We can see that the temperature of the network decreases rapidly when we go from the channel to the bottom of the substrate, it is also observed that the temperature of the network increases with increasing grid polarization. The maximum temperature of the network is 300 K for $V_{gs} = 0$ V and it is 300 K for $V_{gs} = -2$ V.

Figure III.11 illustrates the variation of the network temperature as a function of the polarization of the drain with a base temperature of 300 K and for two polarizations grid ($V_{gs} = 0$ and -2 V). Note that the network temperature increases with increasing gate polarization and hence with increasing V_{ds} . We can say that the maximum temperature corresponding to the hot spot is 300 K for $V_{gs} = 0$ V and $V_{ds} = -2$ V.

Concentration Independent Mobility						
@ Temperature = 300 Kelvin						
		$\mu = 60$				
		$t\mu = 1.5$				
Contacts:						
Name	Num	Work fn	Resist.	Capacit.	Induct.	
		(eV)	(Ohms)	(Farads)	(Henries)	
source	1	3.930	0.000E+00	0.000E+00	0.000E+00	
drain	2	3.930	0.000E+00	0.000E+00	0.000E+00	
gate	3	5.000	0.000E+00	0.000E+00	0.000E+00	
substrate	4	0.000	0.000E+00	0.000E+00	0.000E+00	

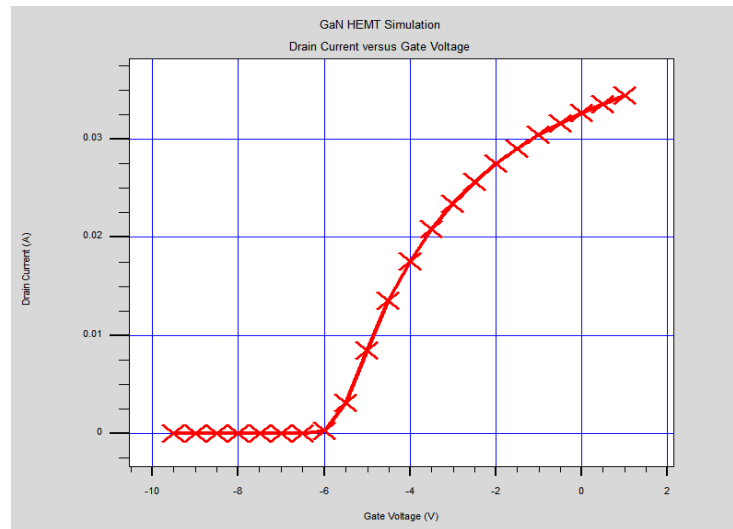


Figure III-11 Effect of geometric parameters on the characteristics of the HEMT to GaN

We note here that the dimensions of the electrodes affect the effectiveness of the device in terms of temperature and current arrival speed, so that DRAIN and SOURCE are identical, and GATE has an upward curve, because DRAIN=GATE = $0.6 * 0.5 \mu\text{m}$ SOURCE = $2 * 0.5 \mu\text{m}$

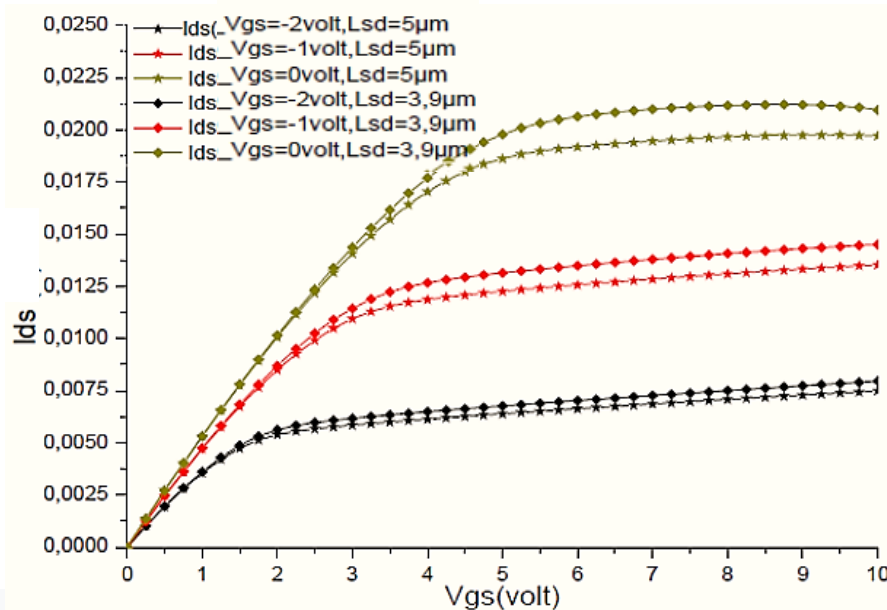


Figure III.12: The variation of the current-voltage characteristics (I_{ds} - V_{ds}) as a function of grid voltage has different grid length.

The variation of the current-voltage characteristics (I_{ds} - V_{ds}) as a function of grid voltage has different grid length.

As can be seen, a relative improvement is designed with the reduction of space drain-source. This is mainly due to the reduction of the input resistances of the source and of drain R_s and R_d which are proportional to the source-gate and gate-drain space like the

$$R_s = R_s + \frac{LSG}{a\mu_p N_d w} \cdot \frac{1}{a}$$

$$R_s = R_s + \frac{LGD}{a\mu_p N_d w} \cdot \frac{1}{a}$$

Where R_c represents the ohmic resistance of the contacts, LSG and LGD is the space between the source and the gate and that of the gate and the drain respectively. a is the channel thickness. μ_p is here permeability of vacuum.

The same observation is reproduced for the I_{ds} - V_{gs} characteristic and the transconductance in function of the voltage of the grid G_m - V_{gs} illustrated by figure III.12.

Effet de la longueur de la grille

Technological parameters play an important role in the optimization and improving the electrical performance of such a structure. In this context, we are interested in studying the influence of the grid length on the current of the drain. Figures III.8-a and III.8-b represent the variation of the drain source current in function of the drain-source voltage V_{ds} for different lengths of the gates L_g (0.5 μm and 0.7 μm) in HEMT AlGaIn / GaN, and without (continuous curves) and with (curves in symbols) thermal effect. It can be seen that the saturation drain current decreases with increasing grid length. Indeed, the lateral extension of the space load zone leads to an elongation of the conductive channel while slimming; which limits the passage of electrons. This means that the more the grid is the longer, the more effective the grid control; on the other hand this causes a increase in the grid source capacity C_{gs} and consequently a degradation of performance in terms of frequencies F_{MAX} (oscillation frequency) and F_T (frequency of transition)

III.7 Conclusion

This chapter introduced the modeling techniques utilized to simulate the AlGa_N/Ga_N HEMT device, the AlGa_N/Ga_N HEMT model developed in this thesis provides a representation of an actual HEMT device that was tested the difficult part of this thesis was making sure there was a suitable HEMT device the parameters examined in this thesis were DC measurements only. one of the the advantages of HEMT are its ability to operate at high frequencies. Would Useful for examining the radio frequency properties of the model developed in this thesis see if the designed device can accurately simulate the frequency and high-power parameters of the actual HEMT device device. Once the basic characteristics are extracted, the device must be simulated in High-frequency and high energy conditions to determine whether the benefits of nitride substrate in the field of alternating current

CHAPTER IV

***Conclusion and future work
prospects***

IV.1 General Conclusion

In our thesis we presented simulation results of AlGa_N/Ga_N HEMT transistors are high performance components. Analyzes the fundamental technical differences of this material and more semiconductors than III-Vs such as gallium arsenide. Its wide range of forbidden energy gallium nitride offers the possibility to produce ternary alloys such as AlGa_N or AlIn_N, making it possible to produce products to manufacture the fastest field transistors.

the structure studied is the structure of HEMT AlGa_N/Ga_N and substrates of the AlGa_N layer that represent formations The donor, followed by a Ga_N channel containing in its upper region, the two-dimensional gas (2DEG) Next come the Ga_N-saved layers. In conclusion, we can state that the output characteristics of HEMT transistor has Ga_N base depend particularly on the polarization of the materials constituting the heterojunction and which are the major source of the interface load. In addition to the grid represents the control electrode for field effect transistors and therefore its dimensions greatly affect the transfer characteristic. Our work and an affirmation of theoretical notions and our results obtained are in agreement with what has been published experimentally or by modeling carried out on heterostructures Ga_N-based HEMT.

We can point out that the study of these transistors requires a lot of learning physics concerning these polarization properties (mechanical) and electronic ones (permittivity, the gap ..ect) and the effect of the dimensions of the grid in terms of height, length, shape and material constituting this electrode

IV.2 Future work prospects

More work is needed on process improvement, device characterization, reliability and circuit integrity until these devices are considered for actual applications.

Power-switching devices require low on-state conduction losses, high-switching speed, high thermal stability, and high input impedance. Using gallium nitride (GaN) based field-effect transistors, these properties for switching devices can be satisfied. GaN-based High Electron Mobility Transistors (HEMTs) are emerging as promising candidates for high-temperature, high-power (power electronics) and radio-frequency (RF) electronics due to their unique capabilities of achieving higher current density, enhancement-mode (e-mode) or normally-off AlGaN/GaN HEMTs are attracting increasing interest in recent years because no negative gate voltage is necessary to turn off the devices. This leads to the advantage of simple circuit design and low stand-by power dissipation. For power electronics applications, power switches which incorporate e-mode devices provide the highly desirable essential fail-safe operation

GaN technology will transform the future

IV.3 - References

- [01] MECHGOUG Amina , simulation d'un transistor algaN/ingaN/gaN a effet de champ (hemt) Université Med Khider Biskra Faculté des Sciences Exactes et des Sciences de la Nature et de la Vie
- [02] . https://en.wikipedia.org/wiki/Gallium_nitride
- [03]. Dalvir K. Saini Wright State University Gallium Nitride: Analysis of Physical Properties and Performance in High-Frequency Power Electronic Circuits 2015
- [04] .Shrawan Jha CENSIS, UK AlGa_N/Ga_N based HEMT structures and applications Article · April 2008
- [05].https://en.wikipedia.org/wiki/Gallium_nitride
- [06] .Li, Hongwei 1975-, "Novel processes for large area gallium nitride single crystal and nanowire growth." (2005). Electronic Theses and Dissertations. Paper 825.
- [07] .https://en.wikipedia.org/wiki/Electronic_band_structure
- [08].https://en.wikipedia.org/wiki/Two-dimensional_electron_gas
- [09]. G. J. Sullivan Rockwell Science Center, Thousand Oaks, California 91358~received 19 January 1999; accepted 3 May 1999!
- [10].B. E. Foutz, M. J. Murphy, The Influence of Spontaneous and Piezoelectric Polarization on Novel AlGa_N/Ga_N/InGa_N Device Structures Published online by Cambridge University Press: 10 February 2011
- [11]. ABDELMOUMENE Mestaria , Etude et modélisation d'un transistor HEMT AlGa_N/Ga_N, Université Abou-Bakr Belkaïd-Tlemcen Faculté de Technologie Département de Génie Electrique et Electronique
- [12]. https://en.wikipedia.org/wiki/Gallium_nitride
- [13].<https://site.unibo.it/semiconductor-physics/en/research/low-dimensional-iii-nitride-alloys-for-high-frequency-electronics>
- [14] .CHIN-PHYS-LETT Growth and Characterization of Modulation Doped Al_xGa_{1-x}N/Ga_N Heterostructures
- [15] Gaudenzio Meneghesso et al 2014 Jpn. J. Appl. Phys. 53 100211 [8] T. Mimura et al., Japn. J. Appl. Phys.19, L225 (1980).

- [16]. https://en.wikipedia.org/wiki/High-electron-mobility_transistor
- [17]. del Alamo, Jesus A. "The High-Electron Mobility Transistor at 30: Impressive Accomplishment and Exciting Prospects." 2011 International Conference on Compound Semiconductor Manufacturing Technology, May 16-19, 2011, Indian Wells, California.
- [18].Tao Sun, Anbang Zhang, Dongfa Ouyang, Siyu Deng, Jie Wei & Bo Zhang Nanoscale Research Letters volume 14, Article number: 191 (2019)
- [19].Stanislav Vitanov Württemberggasse 3 A-1200 Wien, Österreich Matr. Nr. 0527757 geboren am 10. Jänner 1981 in Sofia Wien, im Dezember 2010
- [20].Muhammad Navid Anjum Aadit, Sharadindu Gopal Kirtania, Farhana Afrin, Md. Kawsar Alam and Quazi Deen Mohd Khosru (June 7th 2017). High Electron Mobility Transistors
- [21].P Vimala Dayananda Sagar Institutions Gallium Nitride (GaN) High Electron Mobility Transistors (HEMT) P Vimala Dayananda Sagar Institutions.Shanthi Jeyabal Thiagarajar College of Engineering.High electron mobility transistor-a review on analytical models Article · October 2016
- [22].Muhammad Navid Anjum Aadit, Sharadindu Gopal Kirtania, Farhana Afrin, Md. Kawsar Alam and Quazi Deen Mohd Khosru Submitted: October 27th 2016Reviewed: February 9th 2017Published: June 7th 2017
- [22].Mohammed LAREDJ modélisation électrothermique de transistors en technologie gan montréal, le 25 mars 2011
- [23].SA Kukushkin · 2008 · Cité 196 fois — The best effect has application. SiC and AlN. Unfortunately, the thermal expansion coefficient of Si is more than two times lower as compared to that of GaN, 32 pages
- [24].ABDELMOUMENE Mestaria Etude et modélisation d'un transistor HEMT AlGaN/GaN niversité Abou-Bakr Belkaïd-Tlemcen Faculté de Technologie Département de Génie Electrique et Electronique
- [25].https://compoundsemiconductor.net/article/113362/AlN_Substrates_Show_Much_

Promise_For_GaN_HEMTs

[26] . Anwar Hasan Jarndal Large-Signal Modeling of GaN Device for High Power Amplifier Design

[27] . AYÇA EMEN in partial fulfillment of the requirements for the degree of Master of Science in Micro and Nanotechnology Department, Middle East Technical University by,

[28]. David J. Cheney, Erica A. Douglas, Lu Liu, Chien-Fong Lo, Brent P. Gila, Fan Ren, and Stephen J. Pearton Degradation Mechanisms for GaN and GaAs High Speed Transistors

[29] Gaudenzio Meneghesso et al 2014 Jpn. J. Appl. Phys. 53 100211

[30] MORDI Nasserredine simulation, modélisation et caractérisations électriques des transistors hém^t's

base de composés iii-v nitrurés / faculté de génie électrique département d'électronique soutenue le 17 décembre 2018

[31] ALLAF Mohammed thème étude du comportement du transistor hém^t en hf université mouloud mameri de tizi-ouzou faculté du génie électrique et d'informatique département d'automatique

[32] FARADJI Mohammed Amine modélisation numérique dans le transistor hém^t en technologie gan e de technologie génie électrique et électronique s projet de fin d'études intitulé devant le jury composé d 2012-2013 des effets thermiques

[33] Mr MORDI Nasserredine Simulation, modélisation et caractérisations électriques des transistors HEMT's à base de composés III-V nitrurés

[34] Fetene Mulugeta Yigletu, Sourabh Khandelwal Compact Charge-Based Physical Models for Current and Capacitances in AlGa_N/Ga_N HEMTs,

[35] Sourabh Khandelwal, Nitin Goyal A Physics-Based Analytical Model for 2DEG Charge Density in AlGa_N/Ga_N HEMT Devices,